The Plant Cell, Vol. 23: 3185–3203, September 2011, www.plantcell.org

Function and Evolution of a MicroRNA That Regulates a Ca^{2+}-ATPase and Triggers the Formation of Phased Small Interfering RNAs in Tomato Reproductive Growth [W] [OA]

Ying Wang,[a] Asuka Itaya,[a,1] Xuehua Zhong,[a,2] Yang Wu,[b] Jianfeng Zhang,[a,3] Esther van der Knaap,[c] Richard Olmstead,[d] Yijun Qi,[b] and Biao Ding[a,e,f,4]

[a] Department of Molecular Genetics, Ohio State University, Columbus, Ohio 43210
[b] National Institute of Biological Sciences, 102206 Beijing, China
[c] Department of Horticulture and Crop Science, Ohio State University/Ohio Agricultural Research and Development Center, Wooster, Ohio 44691
[d] Burke Museum, Department of Biology, University of Washington, Seattle, Washington 98195
[e] Molecular, Cellular, and Developmental Biology Program, Ohio State University, Columbus, Ohio 43210
[f] Center for RNA Biology, Ohio State University, Columbus, Ohio 43210

MicroRNAs (miRNAs) regulate a wide variety of biological processes in most eukaryotes. We investigated the function and evolution of miR4376 in the family Solanaceae. We report that the 22-nucleotide miR4376 regulates the expression of an autoinhibited Ca^{2+}-ATPase, tomato (*Solanum lycopersicum*) *ACA10*, which plays a critical role in tomato reproductive growth. Deep phylogenetic mapping suggested (1) an evolution course of MIR4376 loci and posttranscriptional processing of pre-miR4376 as a likely limiting step for the evolution of miR4376, (2) an independent phylogenetic origin of the miR4376 target site in *ACA10* homologs, and (3) alternative splicing as a possible mechanism of eliminating such a target in some *ACA10* homologs. Furthermore, miR4376 triggers the formation of phased small interfering RNAs (siRNAs) from Sl *ACA10* and its *Solanum tuberosum* homolog. Together, our data provide experimental evidence of miRNA-regulated expression of universally important Ca^{2+}-ATPases. The miR4376-regulated expression of *ACA10* itself, and possibly also the associated formation of phased siRNAs, may function as a novel layer of molecular mechanisms underlying tomato reproductive growth. Finally, our data suggest that the stochastic emergence of a miRNA-target gene combination involves multiple molecular events at the genomic, transcriptional, and posttranscriptional levels that may vary drastically in even closely related species.

INTRODUCTION

MicroRNAs (miRNAs) play essential roles in regulating gene expression in most eukaryotes. The biogenesis of miRNAs involves several mechanistic steps. In general, miRNA genes are transcribed into miRNA precursors by the DNA-dependent RNA polymerase II. These precursors are further processed into mature miRNAs that carry out specific biochemical functions in gene regulation. In animals, the long primary transcripts, called primary-miRNAs, are first processed by Drosha and associated protein factors into shorter precursor-miRNAs (pre-miRNAs) in the nucleus, which are then exported into the cytoplasm for subsequent cleavage by Dicer and associated factors into duplexes of miRNA/miRNA* (Kim et al., 2009; Okada et al., 2009). Plants lack Drosha homologs and both processing steps are catalyzed by a Dicer-like enzyme (DCL1) in the nucleus (Park et al., 2002; Reinhart et al., 2002; Kurihara and Watanabe, 2004; Kurihara et al., 2006). In most cases, miRNAs are loaded into the RNA-induced silencing complex to guide cleavage of target mRNAs or repression of translation (Carthew and Sontheimer, 2009; Voinnet, 2009).

In plants, many miRNAs are deeply conserved and abundantly expressed, and they regulate overwhelmingly the expression of transcription factors critical for development or stress responses (Axtell and Bowman, 2008; Axtell, 2008; Chen, 2009). Recent bioinformatics and high-throughput sequencing studies also have uncovered a large number of nonconserved miRNAs, from a green alga to flowering plants, which are species or clade specific. Examples include *Chlamydomonas reinhardtii* (Molnár et al., 2007; Zhao et al., 2007), *Physcomitrella patens* and *Selaginella moellendorffii* (Axtell et al., 2007), *Arabidopsis thaliana* (Lu et al., 2005; Lu et al., 2006; Rajagopalan et al., 2006; Fahlgren et al., 2007; Zhang et al., 2007; Fahlgren et al., 2010), *Arabidopsis lyrata* (de Felippes et al., 2008; Fahlgren et al., 2010; Ma et al., 2010), *Oryza sativa* (Lu et al., 2008; Morin et al., 2008; Zhu et al., 2008; Johnson et al.,

[1] Current address: Agriculture and Agri-Food Canada, 960 Carling Avenue, Building 21, Ottawa, Ontario K1A 0C6, Canada.
[2] Current address: Department of Molecular, Cell, and Developmental Biology, 3218 Life Sciences Building, University of California, Los Angeles, CA 90095.
[3] Current address: Department of Cell and Systems Biology, University of Toronto, 25 Willcocks Street, Room 4055, Toronto, Ontario M5S 3B2, Canada.
[4] Address correspondence to ding.35@osu.edu.
The author responsible for distribution of materials integral to the findings presented in this article in accordance with the policy described in the Instructions for Authors (www.plantcell.org) is: Biao Ding (ding.35@osu.edu).
[W] Online version contains Web-only data.
[OA] Open Access articles can be viewed online without a subscription.
www.plantcell.org/cgi/doi/10.1105/tpc.111.088013

2009), *Pinus contorta* (Morin et al., 2008), *Eschscholzia californica* (Barakat et al., 2007), *Populus trichocarpa* (Lu et al., 2005), *Medicago truncatula* (Szittya et al., 2008; Lelandais-Brière et al., 2009), *Triticum aestivum* (Wei et al., 2009), *Brachypodium distachyon* (Wei et al., 2009), *Solanum lycopersicum* (Moxon et al., 2008), and *Glycine max* (Joshi et al., 2010). Some miRNAs are specific to monocots or dicots (Sunkar and Jagadeeswaran, 2008). A common picture emerging from these results is that these nonconserved miRNAs are expressed at low levels, target diverse genes, exhibit organ- or tissue-specific expression, and may have specialized functions. For instance, the *A. thaliana* miR824, which is conserved in Brassicaceae but is not found outside this family (Rajagopalan et al., 2006; Fahlgren et al., 2007), regulates the expression of *AGAMOUS-LIKE16* that plays a role in controlling stomatal density and development in the leaves (Kutter et al., 2007). Many nonconserved miRNAs, however, have no predictable or validated target genes. A current model postulates that many new miRNAs evolved transiently and, without gaining biological functions, died rapidly through mutational drifts during the course of evolution (Fahlgren et al., 2007, 2010; Ma et al., 2010; reviewed by Axtell, 2008; Axtell and Bowman, 2008; Cuperus et al., 2011). The biological role of the vast majority of nonconserved miRNAs remains unknown, even for many whose targets have been predicted or validated.

We reasoned that experimental and deep phylogenetic analyses of a miRNA and its target gene in a group of organisms with clear phylogenetic relationships could provide unique insights into the biological function and evolution pattern of miRNA-regulated gene expression. In this study, we investigated miR4376 in the family Solanaceae. This family is monophyletic with a well-understood phylogeny tree (Olmstead et al., 2008) and includes some of the most important food, medicinal, and ornamental plants. Here, we present evidence that the 22-nucleotide miR4376 regulates the expression of an autoinhibited Ca^{2+}-ATPase, *ACA10*, which plays a role in tomato reproductive growth. Deep phylogenetic mapping revealed the evolution course of MIR4376 loci in Solanaceae and showed posttranscriptional processing of pre-miR4376 as a likely limiting step during the evolution of miR4376 in some plant species. The mapping further suggested independent phylogenetic origin and possible posttranscriptional modification of the miR4376 target site in *ACA10* homologs. Finally, miR4376 triggers formation of 21-nucleotide phased small interfering RNAs (siRNAs). Together, our study reveals an example of miRNA-regulated expression of universally important Ca^{2+}-ATPases and a novel layer of molecular mechanism underlying tomato reproductive growth. It further suggests posttranscriptional processing as an important control point for the evolutionary emergence of a mature miRNA and for the elimination of its target site in some homologous mRNAs from different plant species. Thus, the stochastic emergence of a miRNA-target gene combination involves multiple molecular events at the genomic, transcriptional, and posttranscriptional levels that may vary drastically in closely related plant species.

RESULTS

Identification of sly-miR4376

We previously identified a 22-nucleotide tomato small RNA, named SlsmR-31a (for *S. lycopersicum* small RNA-31a), by conventional sequencing (Itaya et al., 2008). The same small RNA also was later identified in tomato via deep sequencing by Moxon et al. (2008) and by others (http://smallrna.udel.edu/libraries.php) and summarized (http://ted.bti.cornell.edu/cgi-bin/TFGD/sRNA/sRNA.cgi? sRNA_ID=S0000125). A BLAST search identified the corresponding DNA sequence in one clone (SL1.00ct22836) from chromosome 6 of the completed tomato genome sequence draft (SOL genomics network; http://sgn.cornell.edu, database of Tomato WGS Contigs [SL1.00]), implicating it as a single-copy gene. As shown in Figure 1A, sequence alignment reveals that this small RNA is a homolog of Gma-miR4376 from *G. max* (Joshi et al., 2010). This small RNA also meets several criteria for miRNA discussed below; therefore, it is renamed Sly-miR4376 in this report. First, RNA folding of an in silico transcribed 91-nucleotide sequence containing the sly-miR4376 sequence with mfold (Zuker, 2003) yielded a hairpin (Figure 1B) fitting the structural criteria of a miRNA precursor (Meyers et al., 2008). Furthermore, both sly-miR4376 and gma-miR4376 are derived from the same arms of their respective precursors. In comparison with sly-miR4376, gma-miR4376 has a 1-nucleotide shift toward the 5′ end of its precursor, giving rise to two gaps at both 5′- and 3′-ends and two additional mismatches at positions 16 and 22 (Figure 1A). Second, we found the miR4376-coding sequence in the partial genome sequence of potato (*Solanum tuberosum*) (gb|AC232436.2|), a close relative of tomato. The in silico transcribed potato sequence also folded into a characteristic plant miRNA precursor structure (Figure 1C), suggesting that miR4376 is conserved among close relatives. Based on the available genome sequence data, the miR4376-coding sequence in tomato (http://solgenomics.net/genomes/Solanum_lycopersicum/genome_data.pl) and potato (http://solanaceae.plantbiology.msu.edu) lies within an intergenic region. Finally, the most recent deep sequencing database (http://ted.bti.cornell.edu/) lists sequences matching the miR4376* (tomato small RNA S0086007) (Figure 1B) as well as miR4376 (tomato putative miRNA M00690).

We previously reported a variant of miR4376, differing by an additional nucleotide at the 5′-end of miR4376 (Itaya et al., 2008). These variants appeared to be derived posttranscriptionally from the same MIR4376 locus with extension of a nucleotide at the 5′-end of miR4376. This imprecise processing is consistent with many nonconserved miRNAs found in *A. thaliana* and *A. lyrata* (Ma et al., 2010). Furthermore, the single copy gene for miR4376 also is consistent with the recent evolution of nonconserved miRNAs (Fahlgren et al., 2010; Ma et al., 2010).

RNA gel blots showed high accumulation of miR4376 in leaves and young flower buds but diminished accumulation in young green fruits and near absence from mature fruits (Figure 1D). Detailed analysis showed developmental regulation of miR4376 accumulation in leaves (see Supplemental Figure 1 online).

Cloning and Identification of the miR4376 Target Gene

Initial computational prediction of the miR4376 target was not successful due to lack of the complete tomato genomic sequence when this RNA was first identified. Therefore, we cloned the miR4376 target gene by conventional molecular approaches (see Methods). Briefly, we first cloned a partial sequence of the

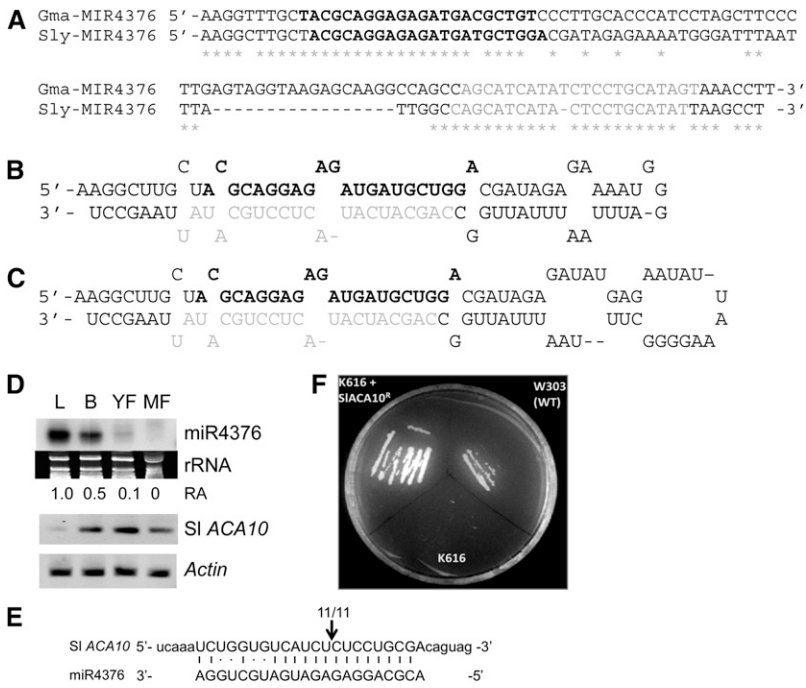

Figure 1. Precursor Structures, Expression Pattern, and Target Validation for miR4376.

(A) Alignment of DNA sequences encoding Gma-miR4376 and Sly-miR4376 from *G. max* and *S. lycopersicum*, respectively. The MIR4376 sequences are highlighted in bold, whereas the MIR4376* sequences are highlighted in light gray. The stars indicate the identical nucleotides between the two species. The Gma-MIR4376–containing sequence was retrieved from Phytozyme (http://www.phytozome.net/) using the Gma-miR4376 precursor sequence from miRBase (http://www.mirbase.org/) as bait. The Create Alignment function in the CLC Free Workbench Software (CLC Bio) was used to align Gma-MIR4376 and Sly-MIR4376, with minor manual adjustment.

(B) and **(C)** Secondary structures of pre-miR4376 from tomato and potato, respectively. The miR4376 and miR4376* sequences are highlighted in bold and light gray, respectively.

(D) Expression of miR4376 and its target gene *ACA10* in different tomato organs. The miR4376 accumulation levels in different organs were analyzed by RNA gel blots and are expressed relative to that in the leaf (arbitrarily set to 1.0). RA, ratio of accumulation levels obtained from two biological replicates. The expression of *ACA10* mRNA was analyzed by RT-PCR, with amplification of *Actin* mRNA as a control. Three biological replicates were performed. L, leaf; B, flower bud; YF, young fruit; MF, mature fruit.

(E) In vivo cleavage site in the 5′-UTR of Sl *ACA10* mRNA as mapped by modified 5′-RACE. The arrow indicates the cleavage site identified in 11 out of 11 clones sequenced.

(F) Complementation of Ca^{2+}-ATPase knockout yeast strain K616 with transfection by Sl *ACA10*^{R}, which is a mutant version of Sl *ACA10* that contains a mutation rendering it resistant to silencing (see text for details of this construct).

miR4376 target gene by 3′-rapid amplification of cDNA ends (RACE). We designed several 3′ RACE forward primers based on the miR4376 sequence, with various truncations at their 3′ ends to circumvent mismatch(s) between the miR4376 and target sequence. Among the forward primers tested, a primer with one nucleotide deletion at the 3′-end allowed cloning of a partial cDNA. Based on the sequence of this partial cDNA, new primers were designed for subsequent 3′- and 5′-RACE to clone the full-length cDNA. The cloned cDNA contains 3246 nucleotides and shares 86% similarity at the amino acid level with *A. thaliana ACA10*, which encodes an autoinhibited Ca^{2+}-ATPase (see Supplemental Figure 2 online). The sequence of this gene was confirmed in the recent tomato genome sequence (http://solgenomics.net). We designate the tomato gene as Sl *ACA10*.

In subsequent searches for additional candidate targets of miR4376 using online prediction software (http://bioinfo3.noble.org/miRNA/miRU.htm) from its default tomato cDNA library, we obtained a fragment (BI932149) belonging to a gene encoding a TCP family transcription factor. However, we were unable to validate this target gene experimentally (see below).

Experimental Validation of the miR4376 Target Gene

Based on the open reading frame prediction by CLC Free Workbench software (CLC Bio), the target sequence of miR4376 resides in the 5′-untranslated region (UTR) of both *ACA10* mRNA and the TCP homolog (BI932149). Using modified RNA ligase-mediated 5′-RACE (Llave et al., 2002; Kasschau et al., 2003), we mapped the cleavage site in *ACA10* at a position opposite to the 9th nucleotide from the 5′-end of miR4376 (Figure 1E). These data establish that miR4376 is a functional miRNA that regulates the stability of *ACA10* mRNA in vivo.

To test whether the cloned *ACA10* encodes a functional Ca^{2+}-ATPase, we performed a complementation test by transforming

the yeast (*Saccharomyces cerevisiae*) triple mutant (*pm1 pmc1 cnb1*) K616 that lacks all Ca^{2+}-ATPases and calcineurin subunit B (Cunningham and Fink, 1994). Complementation of K616 growth has been widely used to demonstrate the Ca^{2+}-transporting functions of various plant Ca^{2+}-ATPases (Geisler et al., 2000; Sze et al., 2000). Our results demonstrated that the tomato gene complemented the growth of K616, indicating that it indeed encodes a Ca^{2+}-ATPase (Figure 1F).

miR4376 Triggered the Formation of Phased siRNAs from *ACA10* Transcripts

Recent studies showed that 22-nucleotide miRNA-mediated cleavage of target transcripts could lead to the production of phased 21-nucleotide siRNAs, depending on the activities of RNA-dependent RNA polymerase 6 and DCL4 in *A. thaliana* (Chen et al., 2010; Cuperus et al., 2010). Such phased siRNAs may function as trans-acting siRNAs to regulate the stability of their target transcripts (Allen et al., 2005; Yoshikawa et al., 2005). Given that miR4376 is 22 nucleotides long, we searched the database containing deep sequencing data of small RNAs from tomato and other plant species (http://smallrna.udel.edu/) for the presence of phased siRNAs from different *ACA10* homologs. Our search using the full-length Sl *ACA10* cDNA sequence as bait uncovered many small RNAs (sRNAs) matching various regions of the cDNA from the leaf, flower, and fruit in both the sense and antisense orientations (see Supplemental Data Set 1 online). We then manually filtered the raw data to identify those sRNAs present in 21-nucleotide registers immediately downstream of the miR4376-mediated cleavage site. As shown in Figure 2, we retrieved a series of phased sRNAs from the pool of total Sl *ACA10*-matching sRNAs. The sense strand sRNAs are designated 3′ P1+, 3′ P2+, 3′ P3+, etc., starting downstream of the 3′-end of Sl *ACA10* cleavage site (Figure 2A). The minus sign following a designee indicates antisense polarity. We refer to them as phased siRNAs in this report, considering their similar pattern with 21-nucleotide phased siRNAs in *A. thaliana*.

Notably, the abundance of phased siRNAs was highest in the leaf, with a decrease in the flower and then in the fruit. This trend is directly correlated with the high-to-low accumulation pattern of miR4376 in these organs (Figure 1D).

In an attempt to find the possible targets of the two most abundant phased siRNAs in tomato, 3′ P2+ and 3′ P5+, we performed computational prediction following the criteria established by Allen et al. (2005). We found several putative candidates as shown in Supplemental Data Set 2 online, with one having the best (but not perfect) match and the others having less convincing matches. None of these putative targets have known or validated functions. Whether any of these are bona fide targets and whether 3′ P2+ and 3′ P5+ indeed regulate the expression of any of these genes to control reproductive growth or other aspects of plant growth remains to be investigated.

We were unable to validate BI932149 by repeated 5′-RACE. Consistent with this observation, we did not find any phased siRNAs, but only one 18-nucleotide sRNA (two reads) matching the BI932149 sequence in the above sRNA database. Therefore, BI932149 may not be a bona fide target gene for miR4376. However, we cannot rule out the possibility that miR4376 mediates a low level of cleavage of this target RNA without producing phased siRNAs or regulates its expression by a mechanism other than cleavage. We also cannot rule out the possibility that unknown technical reasons accounted for our failure to clone the cleavage products.

Disruption of miR4376-Regulated Sl *ACA10* Expression in Transgenic Tomato Specifically Altered Flower Morphology and Fruit Yield

To experimentally test the role of miR4376-regulated *ACA10* expression in tomato, we generated two types of transgenic tomato plants, in which such regulation is perturbed. One type overexpresses miR4376 (miR4376-OX) and the other overexpresses a miR4376-resistant Sl *ACA10* mutant (SlACA10^R-OX) with a FLAG tag, both under the control of the cauliflower mosaic virus (CaMV) 35S promoter. To engineer *ACA10^R*, we altered the miR4376 target sequence 5′-TCTGGTGTCATCTCTCCTGCGA-3′ to 5′-TCTGGTGTCATCT**A**TCCTGCGA-3′, in which the "**A**" substitution for the underlined "C" was predicted to interfere with recognition by miR4376, thereby reducing the efficiency of cleavage, based on findings from studies on other miRNAs (Mallory et al., 2004). Transgenic tomato plants overexpressing green fluorescent protein (GFP) from the same vectors (GFP-OX) served as controls.

We obtained six independent miR4376-OX lines, five SlACA10^R-OX lines, and five GFP-OX lines, all verified to express the transgenes. As an example, shown in Figure 3A, overexpression of miR4376 and *ACA10^R* was verified by RNA gel blots and RT-PCR (in conjunction with sequencing), respectively. GFP expression in the GFP-OX lines was verified by immunoblots (see Supplemental Figure 3A online). In the GFP-OX control plants, miR4376 was detected in sepals and petals, but not in stamen or pistils. This was inversely correlated with the expression pattern of *ACA10* mRNA in these floral parts. In miR4376-OX plants, elevated levels of miR4376 were observed in sepals, petals, the stamen, and pistils, which was correlated with significantly reduced accumulation of *ACA10* mRNA to nearly undetectable levels. In SlACA10^R-OX plants, endogenous *ACA10* had a similar expression pattern as in GFP-OX plants. Expression of *ACA10^R* was higher in sepals, petals, and stamens compared with that of endogenous *ACA10*, as expected of reduced efficiency of miR4376-mediated cleavage. Expression of this mutant was additionally verified by immunoblots using anti-FLAG antibodies (see Supplemental Figure 3B online). The protein band size suggests that the dimeric form of ACA10 was present. Whether this is the functional form of ACA10 remains to be determined; however, previous studies have demonstrated that Ca^{2+}-ATPases exist and function as homodimers (Basu and Briskin, 1995; Sackett and Kosk-Kosicka, 1996; Ushimaru and Fukushima, 2008).

Neither the miR4376-OX nor the SlACA10^R-OX plants exhibited obvious differences in seed germination, height, or leaf morphology in comparison with the GFP-OX lines (see Supplemental Figure 4 online). The first notable and consistent phenotype of miR4376-OX and SlACA10^R-OX plants was an increased vertical distance between the anther and stigma compared with GFP-OX plants (Figure 3B). The other floral organs appeared not to be affected. Quantitative analysis showed that the increased anther-stigma distance was attributed to elongated stamen filaments (see Supplemental Figure 5 online).

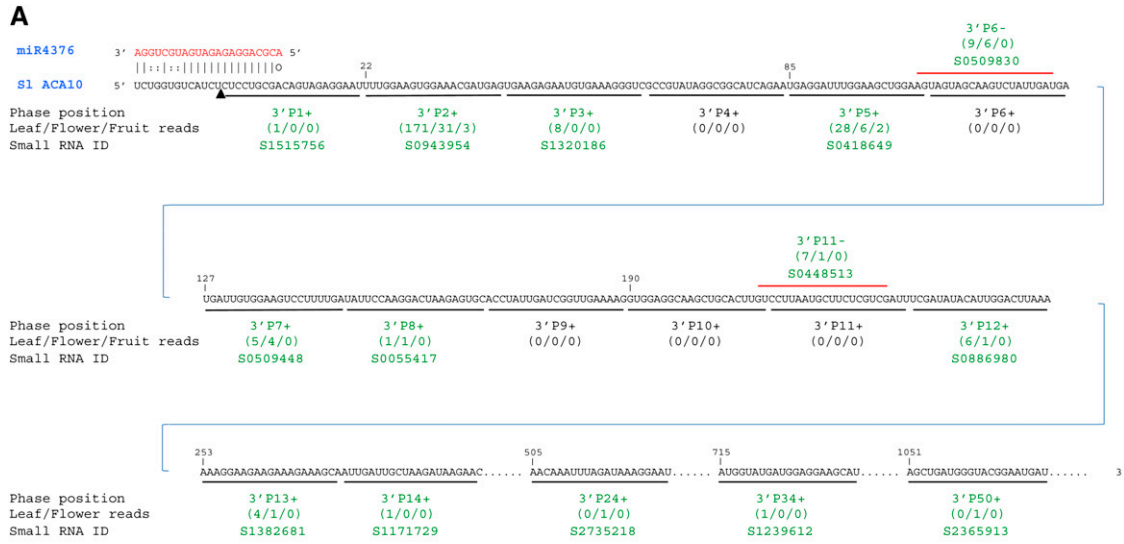

Distribution of Sl *ACA10*-matching siRNAs of various lengths

Organ	Total reads	18 nt	19 nt	20 nt	21 nt total	21 nt phased	22 nt	23 nt	24 nt	25 nt
Leaf	679	1	5	8	606	242	55	4	0	0
Flower	138	2	1	4	114	53	16	0	0	1
Fruit	18	0	0	1	13	5	4	0	0	0

Figure 2. Phased siRNAs Derived from *ACA10* in Tomato Based on Searches in the sRNA Deep Sequencing Database (http://smallrna.udel.edu/).

(A) Phased pattern of 21-nucleotide siRNAs along the Sl *ACA10* sequence. The sense strands of phased siRNAs are designated 3′ P1+, 3′ P2+, 3′ P3+, etc., starting from the validated miR4376-cleavage site that is marked by an arrowhead. Two antisense siRNAs (3′ P6- and 3′ P11-) are shown above the *ACA10* sequence (indicated by red lines). The nucleotide positions are indicated above the sequence, with the nucleotide immediately downstream of the cleavage site designated as "1" (not shown for image clarity). Green indicates siRNAs found in the above deep sequencing database. The rest of predicated phased siRNAs were not found for any organs in the database. The read number of each siRNA in the leaf/flower/fruit is presented in parenthesis. The ID of each siRNA (or sRNA) in the Tomato Functional Genomics Database (http://ted.bti.cornell.edu/) is given.

(B) Distribution of *ACA10*-matching sRNAs of various lengths in the leaf, flower, and fruit of tomato. The numbers in the "21 nt total" column represent the total reads for each of the tomato organs, whereas those in the "21 nt phased" column represent subsets from the 21-nucleotide total reads.

The most significant impact of miR4376 or *SlACA10^R* overexpression was drastically reduced yield of mature fruits (Figure 3C). The six miR4376-OX lines each produced a similar number of flowers as the five GFP-OX control lines (Table 1). However, they produced zero to six mature fruits, in contrast with the GFP-OX control lines that produced 20 to 42 mature fruits (except for one line that produced six) (Table 1). SlACA10^R-OX plants also had similar number of flowers as the GFP-OX plants but reduced number of mature fruits like miR4376-OX plants (Table 1). The mature fruits from the transgenic lines did not exhibit differences in size or morphology. Close examination showed many small green fruits that failed to grow into mature fruits in both miR4376-OX and SlACA10^R-OX transgenic plants (see Supplemental Figure 6 online). For example, we observed 36 and 40 such small fruits in two miR4376-OX plants and 28 and 34 such fruits in two SlACA10^R-OX plants.

It was surprising that miR4376-OX and SlACA10^R-OX plants exhibited similar, rather than opposite, phenotypes. A simple explanation is that a particular level of *ACA10* expression in tomato flowers and fruits is critical for reproductive growth and that altered expression to levels lower or higher than the optimal would cause similar phenotypes. There are prior examples where up- and downregulated expression of a gene can lead to a similar phenotype. These include the genes encoding BRI1-ASSOCIATED RECEPTOR KINASE1 (BAK1) in *O. sativa* (Wang et al., 2007a; Li et al., 2009), *N*-METHYL-D-ASPARTASE (NMDA), a subtype of Glu receptors, in animals (reviewed in Hardingham and Bading, 2003), and CALCINEURIN (CN) in *Caenorhabditis elegans* (Ahn et al., 2006). BAK1 is involved in brassinosteroid signaling, and plants exhibited a similar dwarf phenotype when *BAK1* was upregulated or downregulated. It is noteworthy that NMDA receptors and CN are probably involved in Ca^{2+} signaling. Up- or downregulation of NMDA receptors is toxic to neurons, and up- or downregulation of CN in *C. elegans* led to similar slow growth and a reduction in reproduction.

It is important to note that the transgenic expression of miR159 under the control of the CaMV 35S promoter in tomato led to pleiotropic phenotypes, including developmental defects in leaves, flowers, and fruits (Buxdorf et al., 2010). By contrast, there were no observable phenotypes for vegetative growth in our

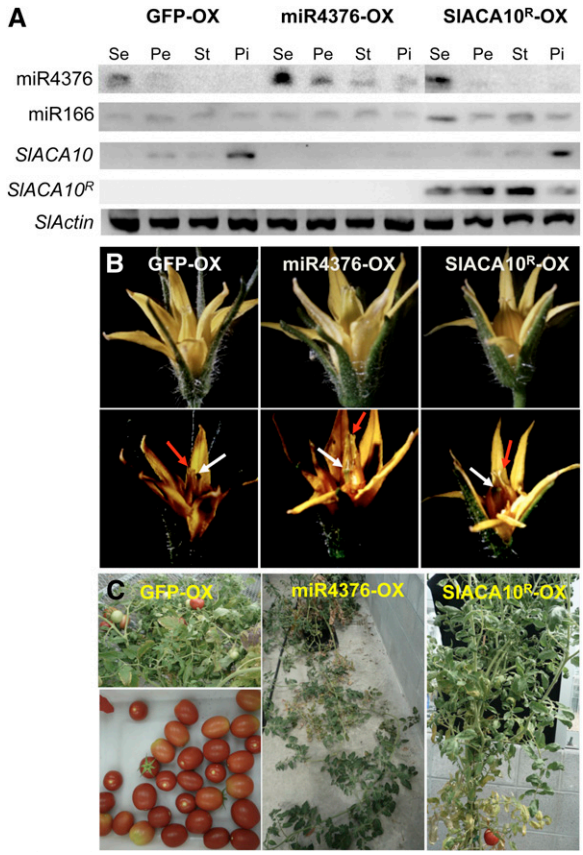

Figure 3. Transgenic Overexpression of miR4376 or the Cleavage-Resistant *ACA10* Mutant (*ACA10*^{R}) Affects Flower Morphology and Fruit Yield in Tomato.

(A) Expression patterns of miR4376 (by RNA gel blots), *ACA10*, and *ACA10*^{R} mRNA (by RT-PCR) as well as control *Actin* mRNA in different floral organs of all transgenic lines. Three biological replicates were performed for each transgenic line.

(B) The top panels show indistinguishable flower morphology among GFP-OX, miR4376-OX, and SlACA10^R-OX lines. The bottom panels show enhanced vertical distance between the anther (red arrow) and stigma (white arrow) in miR4376-OX and SlACA10^R-OX lines in contrast with that in the control GFP-OX line, when the stamen is partially dissected.

(C) Transgenic overexpression of miR4376 or the cleavage-resistant *ACA10* mutant (*ACA10*^{R}) drastically reduces fruit yield in tomato.

miR4376-OX and SlACA10^R-OX transgenic plants in comparison with the controls, although the same CaMV 35S promoter was used. Thus, the abnormal flower and fruit phenotypes of our transgenic plants suggest a predominant role of miR4376-regulated *ACA10* expression in normal tomato reproductive growth.

miR4376 Appears to Be More Prevalent in Solanaceae

Considering the ubiquitous presence and critical biological roles of Ca^{2+}-ATPases in various organisms (Sze et al., 2000; Carafoli, 2002) and lack of previous reports on miRNAs regulating these genes, we addressed the question of how widespread miR4376 is in plants so as to develop a basis for further investigations on its role in plant growth and development. A BLAST search of miRNA databases did not find the exact match of the miR4376 sequence in plant species outside the Solanaceae family, such as *A. thaliana*, *O. sativa*, and *P. trichocarpa* as well as the unicellular green alga *C. reinhardtii* (http://www.mirbase.org/). The miR4376-coding sequence was also absent from the genome sequences of *A. thaliana* (http://www.Arabidopsis.org/Blast/), *P. trichocarpa* (http://genome.jgi-psf.org/Poptr1_1/Poptr1_1.home.html), *Vitis vinifera* (http://www.genoscope.cns.fr/cgi-bin/blast_server/projet_ML/blast.pl), *O. sativa* (http://blast.jcvi.org/euk-blast/index.cgi?project=osa1), *Zea mays* (http://www.maizesequence.org/blast), and *C. reinhardtii* (http://www.chlamy.org/cgi-bin/webblast.pl).

Besides the search for exact matches, we also searched for similar miRNAs in the miRBase (http://www.mirbase.org/) and in the database of comparative sequencing of plant sRNAs (http://smallrna.udel.edu) (Mahalingam and Meyers, 2009) by allowing up to four mismatches (including gaps) (Meyers et al., 2008). As discussed earlier, the miR4376 from *G. max* (Joshi et al., 2010) was identified in such search. Additional search result is summarized in Supplemental Data Set 3 online. The *G. max ACA10* transcripts do not have the miR4376 target site (see Supplemental Figure 14 online). The target gene of *G. max* miR4376 remains to be identified and validated.

In the plant sRNA database (http://smallrna.udel.edu), we found one sRNA sequence (ID3 in Supplemental Data Set 3 online) that has one mismatch with miR4376 (A versus G at position 17 for ID3 and miR4376, respectively). This sRNA is present in petunia (*Petunia hybrida*) flower (14 out of 2,537,548 reads), grapevine flower (1 out of 2,208,760 reads), and *Setaria italica* root (1 out of 4,392,037 reads). This sRNA has not been validated as a miRNA. When we cloned *MIR4376* from petunia (see primer designs and cloning strategy below), we had 6/6 clones showing G at position 17 and did not recover any clones with A at this position. Thus, we could not determine if this petunia sRNA (i.e., ID3) read is derived from the *MIR4376* loci or from another genomic locus. For grapevine and *S. italica*, we could not find the exact match in their genome sequences except for some fragments with several mismatches (http://www.phytozome.net). Thus, we are unable to determine the nature of this sRNA, given (1) its extremely low read numbers from deep sequencing, (2) the mismatch with miR4376, and (3) unfound match in the currently available genome sequences. In summary, at this stage, we have not been able to conclude with confidence the presence or absence of miR4376 homologs elsewhere through our expanded database searches.

Considering that *A. thaliana*, *P. trichocarpa*, and *V. vinifera* are representatives of Rosidae (Chase and Reveal, 2009) (see Supplemental Figure 7 online), miR4376 appears to be absent from at least some species of Rosidae. Tomato belongs to the Asteridae subclade Lamiidae. To test whether miR4376 is present in the Asteridae subclade Campanulidae, the sister group to Lamiidae, we used PCR (see primer designs below and in Methods) to determine whether the DNA sequence encoding miR4376 was present in *Chrysanthemum cinerariifolium*, a member of the Campanulidae subclade. Indeed, the result was positive (see Supplemental Figure 8 online).

Table 1. Flower and Mature Fruit Counts in Different Transgenic Lines

Construct	1	2	3	4	5	6	Average
GFP-OX	32 (361)	24 (352)	20 (358)	42 (362)	6 (323)		24.8 (351.2)
miR4376-OX	1 (303)	1 (339)	6 (321)	6 (321)	1 (311)	0 (318)	2.7 (322.2)
SlACA10^{R}-OX	7 (355)	8 (349)	6 (348)	1 (331)	4 (350)		5.2 (346.6)

The first row indicates different transgenic lines expressing each of the constructs indicated in the first column. The data show the number of mature fruits from each line, with the number of flowers given in parentheses.

Overall, our current data suggest that miR4376 does not appear to be deeply conserved in all taxonomic groups of plants. Further investigations, especially with the increasing availability of genome sequences of more plant species, may help improve knowledge of the taxonomic group distribution of miR4376 in plants. In subsequent studies, we focused on the phylogenic mapping of miR4376 origin in Solanaceae and closely related plants.

Deep Phylogenetic Mapping Showed Random Occurrence of miR4376 in Solanaceous Species

When using RNA gel blots to confirm the expression of miR4376, we detected the presence of mature miR4376 in tomato but not in *A. thaliana*, as expected. Surprisingly, we did not detect miR4376 accumulation in two other solanaceous species, *Nicotiana benthamiana* and *Nicotiana tabacum* (see Supplemental Figure 9 online). This invoked the question of how miR4376 evolved in the family Solanaceae. Based on the current phylogeny tree of Solanaceae (Olmstead et al., 2008), we selected the following species to trace the evolution of miR4376: *Goetzea elegans*, *Calibrachoa hybrida*, *P. hybrida*, *N. tabacum*, *N. benthamiana*, *Brugmansia aurea*, *Whithania somnifera*, *Iochroma cyaneum*, *Physalis franchetii*, *Capsicum baccatum*, *Capsicum annuum*, *Jaltomata procumbens*, and *Solanum melongena* (eggplant). Tomato and potato served as positive controls. These species are shown in Figure 4 according to their phylogenetic relationship (Olmstead et al., 2008). All species above *P. hybrida* belong to the X=12 clade. These species represent the major suprageneric groups in Solanaceae, including Goetzeoidae, Petunieae, Nicotianoideae, Datureae, Withaninae, Iochrominae, Physalinae, Capsiceae, and Solaneae (Olmstead et al., 2008). We also included *Ipomoea batatas* of Convolvulaceae, a sister group of Solanaceae, and *Gardenia jasminoides* (Rubiaceae, Gentianales), a more distantly related species of Lamiidae (Olmstead et al., 2000).

Because of the lack of genomic and RNA sequence information for most of the selected species, we combined traditional molecular cloning methods and bioinformatics, wherever relevant, in our analysis. We performed RNA gel blotting with total RNA samples from flowers and young leaves from such flowering plants, respectively, to examine the presence of miR4376 in each species, with three to five biological replicates. We used the deeply conserved miR166 (Floyd and Bowman, 2004) as a positive control. As shown in representative RNA gel blots in Figure 5 and summary data in Figure 4, we could detect the accumulation of mature miR4376 in most species but not in *I. batatas*, petunia, tobacco, *N. benthamiana*, and eggplant. Consistent with our RNA gel blot data, the publicly available database of deep sequencing results for sRNAs from various plant species (http://smallrna.udel.edu/project_data.php) shows absence of sRNA sequence matching miR4376 from petunia, very low read numbers in tobacco leaves (109), and high read numbers in leaves of *C. annuum* (2617), potato (2192), and tomato (3791) (see Supplemental Table 1 online). These data indicate that the level of accumulation of mature miR4376 is species dependent in Solanaceae.

Deep Phylogenetic Mapping Enabled Tracing of the Evolution Path of *MIR4376* Loci

The absence of miR4376 in *I. batatas* (as determined by RNA gel blot), petunia (RNA gel blot and deep sequencing), *N. benthamiana* (RNA gel blot), and eggplant (RNA gel blot) raised the question of whether the miR4376-coding sequence was absent from these plants. To address this question, we used PCR to amplify the miR4376-coding sequence from the genomes of all test species, using primers designed based on the DNA sequences flanking and including partial miR4376 and miR4376* sequences. To facilitate primer design, we first found two identical tobacco DNA clone sequences of ~480 bp, which contain the sequence encoding a perfect miR4376 near the center, in the NCBI BLAST genomic survey sequence (gb|FH484005.1| and gb|FH483922.1|). As shown in Supplemental Figure 10 online, the tobacco sequence has significant similarity with the tomato and potato sequences, with many regions of identical sequences. Furthermore, deep sequencing showed that miR4376/miR4376* sequences from *C. annuum* were identical to those of tobacco, tomato, and potato (http://smallrna.udel.edu/). Based on these observations, we postulated that the miR4376/miR4376* region and immediate flanking sequences should be highly conserved, even with possible small sequence variations, in the solanaceous and related species. Thus, a common set of primers should permit us to amplify the precursor sequences from these species. Specifically, as shown in Supplemental Figure 10 online, the primer sequences cover nucleotides 1 to 10 of the miR4376 sequence and nucleotides 1 to 21 of the miR4376* sequence. We isolated genomic DNA from each species as PCR template. We amplified and sequenced miR4376-containing sequences in all species. These findings are summarized in Figure 4. As a control, no product was amplified from *A. thaliana* genomic DNA. These data indicate that the miR4376-coding sequences are present in all solanaceous plants and the two related species.

We then compared the predicted secondary structures of RNAs computationally transcribed from the cloned sequences, which are operationally referred to as miR4376 precursors (pre-miR4376). All predicted structures are shown in Figure 4, with the

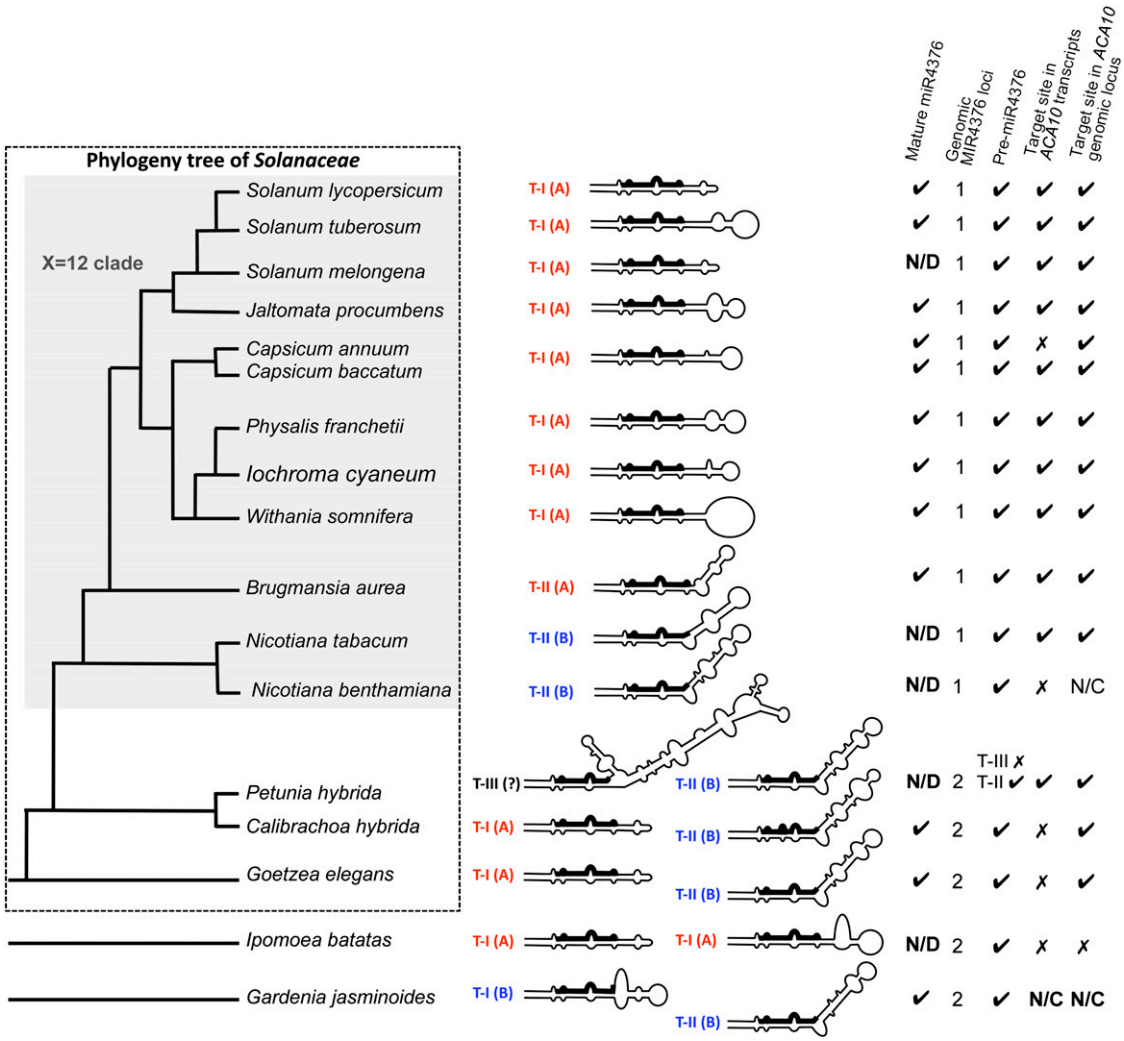

Figure 4. Deep Phylogenetic Mapping of miR4376 and Its Target Site Evolution in Solanaceae and Related Species.

Left panel shows a simplified view of the current phylogeny tree of Solanaceae (Olmstead et al., 2008). The middle panel shows the predicted secondary structures of in silico transcribed pre-miR4376 sequences from various species. The bold line indicates the position of the mature miR4376 sequence. T-I, T-II, and T-III denote Type I, Type II, and Type III secondary structures of pre-miR4376 transcripts, respectively. The red A and blue B following a Type indicate Version A and Version B MIR4376 loci, respectively. The right panel summarizes data showing the presence or absence of mature miR4376, genomic MIR4376 loci, pre-miR4376 transcripts, and the miR4376 target sites in *ACA10* mRNA transcripts and in genomic *ACA10* loci of various species in Solanaceae and close relatives. N/C, not conclusive due to technical problems; N/D, not detectable.

miR4376 position highlighted as a thicker line (see Supplemental Figure 11 online for the sequences of all the folded structures). These secondary structures could be classified into three broad types: Type I (T-I), which was nearly rod-shaped; Type II (T-II), which contained a sharp turn at the 3′-end of miR4376; and Type III (T-III), which was branched at the 3′-end of miR4376. While the secondary structures of stem regions containing miR4376 were similar for these different types, the regions distal to the 3′-end of miR4376 were variable for the number of loops and secondary structures, with the pre-miR4376 of eggplant and tomato having the simplest and a similar structure (see Supplemental Figure 11 online). Interestingly, all tested species in the X=12 clade had one type of secondary structure (Type I or II), whereas the remaining species of Solanaceae each had two types. Notably, the tomato cloning result is consistent with the genome sequence data showing a single copy gene, supporting the validity of the cloning results for all species.

Analysis of the nucleotide sequences of stem/loop regions, using the CLC Free Workbench software, offered some indication of shared ancestry. As shown in Figure 6, sequence alignment suggests the existence of two main versions of *MIR4376* genes, which we call Version A and Version B. These versions are indicated as red A or blue B following a specific secondary structure type [e.g., T-III (A)] in Figure 4 and have version-specific sequences outside the *MIR4376*/*MIR4376** pair. As discussed above, we assume that any sequence variations in the *MIR4376*/

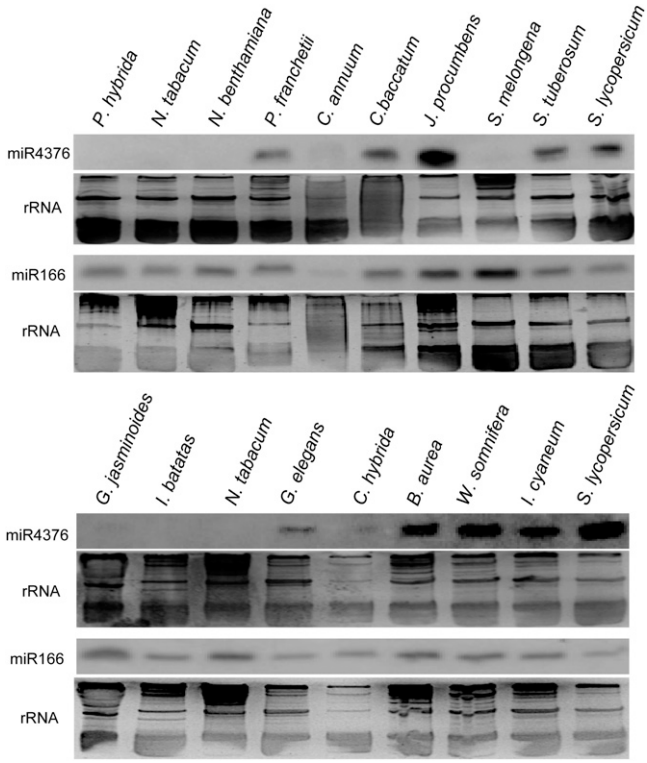

Figure 5. RNA Gel Blots Showing Accumulation of Mature miR4376 in Various Plant Species.

sRNAs were extracted from the leaves of plants at the flowering stage. The sample from each plant was divided equally into two halves and run on a 17% (w/v) polyacrylamide/8 M urea gel for hybridization with miR4376- and miR166-specific probes, respectively. The deeply conserved miR166 was used as an internal control. Ethidium bromide staining of rRNA shows loading controls.

*MIR4376** pair in other species are likely small enough not to alter the overall sequence conservation. The sequence similarities in the non-miRNA stem/loop region within each of these two versions are so strong that it is unlikely that they evolved convergently. Version A includes all *Solanum*, *Jaltomata*, *Capsicum*, *Physalis*, *Iochroma*, *Withania*, and *Brugmansia* copies, the copy labeled Type I in *Calibrachoa* and *Goetzea*, and both copies in *Ipomoea*. Version B includes copies in the two *Nicotiana* species, the *Petunia*, *Calibrachoa*, and *Goetzea* Type II copies, and both copies of *Gardenia*. This classification implies that the unique curved secondary structure of Version A in *Brugmansia* arose independently. The two *Gardenia* stem/loop secondary structures may superficially look different, but they share 25 of the first 30 nucleotides (through the stem to the terminal loop on each).

The very large precursor in *Petunia* (Type III) did not exhibit any evident homology to either Version A or Version B locus in its stem/loop sequence. It is either an aberrant Version A copy that has obtained a large novel stem/loop region or is a novel sequence entirely.

This pattern suggests that both versions found in Solanaceae (e.g., in *Goetzea* and *Calibrachoa*) existed in the most recent common ancestor of Rubiaceae (*Gardenia*) and Solanaceae but that in the lineage leading to *Gardenia*, Version A was lost and Version B was duplicated, whereas in the lineage leading to *Ipomoea*, Version B was lost and Version A was duplicated. In Solanaceae, both were retained in the early diversification of the family. However, only Version B was retained in *Nicotiana*, and Version A was retained in subfamily Solanoideae. Since *Calibrachoa* is sister to *Petunia* and has both versions, it might be most parsimonious to assume that Version A was transformed into Type III in *Petunia* or that it was lost and replaced with a new locus.

Some Pre-miR4376 Transcripts Were Weakly or Not Processed into Mature miR4376

The absence of miR4376 from *I. batatas*, petunia, *N. benthamiana*, and eggplant as well as low accumulation in tobacco, in contrast with the presence of miRNA-coding sequences in all of these species, raised the question of whether the DNA sequences were transcribed in these species or transcript levels were low in comparison with other species. To address this question, we isolated total RNAs from the leaves and flowers, separately, from each of all test plant species for RT-PCR using the same primer set as used for genomic DNA sequence amplification. The amplification reaction with *A. thaliana* RNA template using the same primer set served as a negative control, and the amplification reaction with 5S rRNA template using 5S rRNA-specific primers served as an internal positive control. The RT-PCR product was sequenced for each species (except for the controls). Examples of RT-PCR results are shown in Figure 7. All data are summarized in Figure 4, based on results from at least three biological replicates for each species. These data revealed several interesting findings. First, the predicted Type III transcripts were absent from petunia, in contrast with the presence of Type II transcripts, suggesting that the Type III DNA sequence was not transcribed or transcribed at a level below detection by our method. Second, pre-miR4376 accumulated to similar levels in tobacco and in tomato, suggesting that the low accumulation of mature miR4376 in the former was likely the result of poor processing of the precursor. Third, the eggplant pre-miR4376 level was low (the same pair of primers for genomic cloning did give a reasonable amount of cloning product), which may account for the low accumulation of mature miR4376 in this plant. The low accumulation of eggplant pre-miR4376 suggests reduced transcription activity of *MIR4376* gene during evolution.

Deep Phylogenetic Mapping Revealed the Random Appearance of the miR4376 Target Site in *ACA10* Homologs at the DNA and mRNA Levels

To gain further insight into the evolution of miR4376-regulated *ACA10* expression, we analyzed the presence of the miR4376 target site in *ACA10* homologs from all test species. First, we searched genome databases and EST collections (National Center for Biotechnology Information; http://blast.ncbi.nlm.nih.gov/bl2seq/wblast2.cgi). Second, if there was no genomic or EST information for a species, we used 5′-RACE to clone the partial 5′-UTRs of mRNA sequences expected to cover the target site region (see flow chart in Supplemental Figure 12

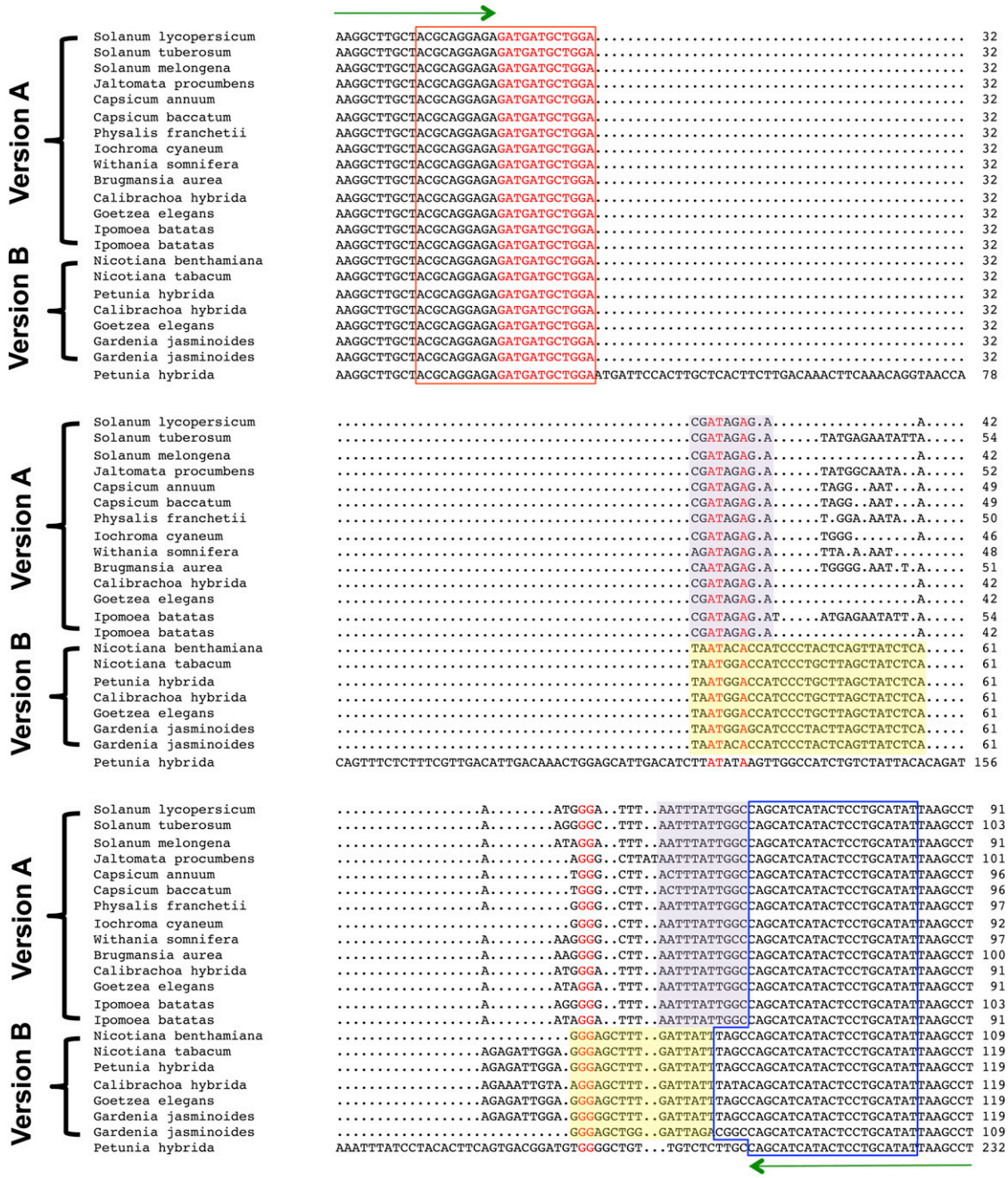

Figure 6. Alignment, Using CLC Free Workbench Software, of Sequences Corresponding to the Cloned Genomic MIR4376 Genes in the Test Solanaceous Species *I. batatas* and *G. jasminoides*.

The alignment result shows two versions of MIR4376 genes, named Version A and Version B. Conserved nucleotides in all species are in red. Sequences corresponding to mature miR4376 and miR4376* are highlighted in a red box and blue box, respectively. The green arrows indicate primer sequences used for the cloning of pre-miR4376. The primer sequences were designed based on the known conserved sequences in tomato, potato, and tobacco. The relatively conserved regions for Version A and Version B are highlighted in purple and yellow, respectively.

online). The exact match of the miR4376 target site in *ACA10* mRNA was found only in some solanaceous species (Figure 8). All partial mRNA and EST sequences are shown in Supplemental Figure 13 online. The data are summarized in Figure 4 and Supplemental Table 2 online, in which presence of the target site in the genomic DNA is inferred by its presence in the mRNA.

Unexpectedly, the miR4376 target site was absent from the cloned *ACA10* mRNA homolog transcripts of *G. elegans*, *C. hybrida*, and *C. annuum* as well as from the EST sequence of *N.*

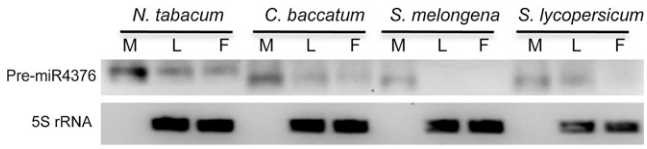

Figure 7. RT-PCR Revealing the Accumulation of Pre-miR4376 Transcripts in Several Species as Examples.

For each species, RNA samples were collected from flowers and young leaves at the flowering stage of plants. 5S rRNA served as an internal control. Three biological replicates were performed for each species. M, genomic fragment that was PCR amplified with the same primers used for RT-PCR and sequenced, used here as size markers for the RT-PCR product; L, leaf; F, flower.

benthamiana (EST759881), despite the presence of *MIR4376* gene in these plants. In particular, *G. elegans*, *C. hybrida*, and *C. annuum* accumulated mature miR4376. On the other hand, the cloned *ACA10* mRNA homologs of *P. hybrida*, *N. tabacum*, and *S. melongena* have a perfect miR4376 target site despite the absence or negligible level of miR4376 mature miRNA in these plants.

The absence of a miR4376 target site from the *ACA10* homolog transcripts of *G. elegans*, *C. hybrida*, and *C. annuum*, in contrast with the accumulation of mature miR4376 in these plants, raised the question of whether the target site was absent from the genomic sequences of *ACA10* in these plants. To address this question, we cloned the genomic fragment flanking the predicted miR4376 target site for sequencing (see flow chart in Supplemental Figure 12 online for cloning strategy). The sequencing results revealed a perfect or near-perfect miR4376 target site in the 5′-UTRs of *ACA10* homologs in *G. elegans*, *C. hybrida*, and *C. annuum* (Figure 8). The cloned DNA sequences are shown in Supplemental Figure 14 online. At least four clones sequenced from leaf samples of flowering *G. elegans* and *C. hybrida* plants, respectively, and two clones sequenced from a flowering *C. annuum* plant were all identical. One plausible explanation is that the miR4376 target site is embedded in an intronic sequence, as illustrated in Figure 8 and Supplemental Figure 14 online, that is lost in mature *ACA10* mRNA due to splicing of pre-mRNAs in these species. As a control of PCR experiments, we amplified the expected *ACA10* DNA sequence from *P. hybrida* (Figure 8; see Supplemental Figure 14 online).

As discussed earlier, miR4376-mediated cleavage of Sl *ACA10* led to the production of phased siRNAs, and the abundance of phased siRNAs is positively correlated with the abundance of miR4376. To further test the direct correlation between potential miR4376-mediated *ACA10* cleavage and phased siRNA production, we searched the sRNA database (http://smallrna.udel.edu/) for the presence of possible *ACA10*-derived phased siRNAs from other solanaceous species, including potato, *C. annuum*, tobacco, and *P. hybrida*, for which the sRNA sequences are available. As shown in Supplemental Data Set 1 and Supplemental Figure 15 online, we detected *ACA10*-derived phased siRNAs from potato. However, as shown in Supplemental Data Set 1 online, we did not detect any phased siRNAs derived from the known partial *ACA10* sequences in the other species (see Supplemental Figure 13 online for these sequences). Thus, the presence of *ACA10* phased siRNA in potato is positively correlated with the presence of both miR4376 and its cleavage site in potato *ACA10*. The absence of phased siRNAs from *C. annuum*, tobacco, and *P. hybrida* may well be accounted for by the observations that (1) *ACA10* transcripts in *C. annuum* do not possess the miR4376 target site, (2) miR4376 has a low read number in tobacco, and (3) miR4376 was not detected in *P. hybrida* by either deep sequencing or RNA gel blots. All together, our data suggest the possibility that generation of *ACA10* phased siRNAs is triggered by miR4376-mediated cleavage, reminiscent of the miRNA cleavage-dependent generation of phased siRNAs in *A. thaliana* (Montgomery et al., 2008). Our data further support the notion that, in Solanaceae, miR4376-mediated *ACA10* expression as well as phased siRNA production evolved in a species-dependent manner in Solanaceae.

Our data suggest that the miR4376 target site in *ACA10* evolved independently of miR4376. As further support of this possibility, our BLAST searches showed several species outside the Solanaceae to have a similar, but not identical, miR4376 target sequence in their *ACA10* homologs. These species included *I. batatas* (cloned), *Helianthus annuus* (DY904876), *A. thaliana* (At4g29900), *P. trichocarpa* (XM_002325215), *V. vinifera* (XM_002262793.1), *G. max* (Glyma17g06520), and *O. sativa* (Os04g0605500) (see Supplemental Figure 16 online). Interestingly, analysis of available genomic and cDNA sequences for these species shows annotated introns that include miR4376 target site-like sequences in *G. max* and *V. vinifera* (see Supplemental Figure 14 online), which supports the view that the miR4376 target site is lost due to splicing in *G. elegans*, *C. hybrida*, and *C. annuum*. These data also suggest that the miR4376 target site in *ACA10* was present before the divergence of dicots and monocots. However, at this stage, we cannot formally rule out the possibility that miR4376 evolved from *ACA10* sequences via inverted gene duplication (Allen et al., 2004).

DISCUSSION

A New Mechanism of miRNA-Regulated Ca^{2+} Signaling

Our work provides direct experimental evidence of miRNA-regulated expression of a plant Ca^{2+}-ATPase. This likely has broad implications in light of the ubiquitous role of Ca^{2+} signaling and the conserved nature of Ca^{2+}-ATPases in plants and other organisms (Sanders et al., 1999, 2002; Sze et al., 2000; Carafoli, 2002; Hepler, 2005; Boursiac and Harper, 2007; McAinsh and Pittman, 2009; Dodd et al., 2010; Kudla et al., 2010). Ca^{2+} signatures, or oscillations, in the cytoplasm or organelles are critical for signal transduction and are regulated by influx through the activities of Ca^{2+} channels and efflux through the activities of high affinity Ca^{2+}-ATPases (pumps) or low-affinity Ca^{2+} exchangers (McAinsh and Pittman, 2009; Dodd et al., 2010; Kudla et al., 2010). There are 14 Ca^{2+}-ATPases in *A. thaliana* and *O. sativa*, which indicates broad conservation, with four being endoplasmic reticulum–type Ca^{2+}-ATPases and 10 being ACAs (Baxter et al., 2003). The 10 ACAs are grouped into four clusters, based on sequence alignments and intron positions, and *A. thaliana ACA10*, *ACA8*, and *ACA9* are clustered together (Baxter et al., 2003). ACA8 (Bonza et al., 2000) and ACA9 (Schiøtt et al., 2004) are localized to the plasma membrane. ACA10 may be similarly localized, given its predicted structural similarity with

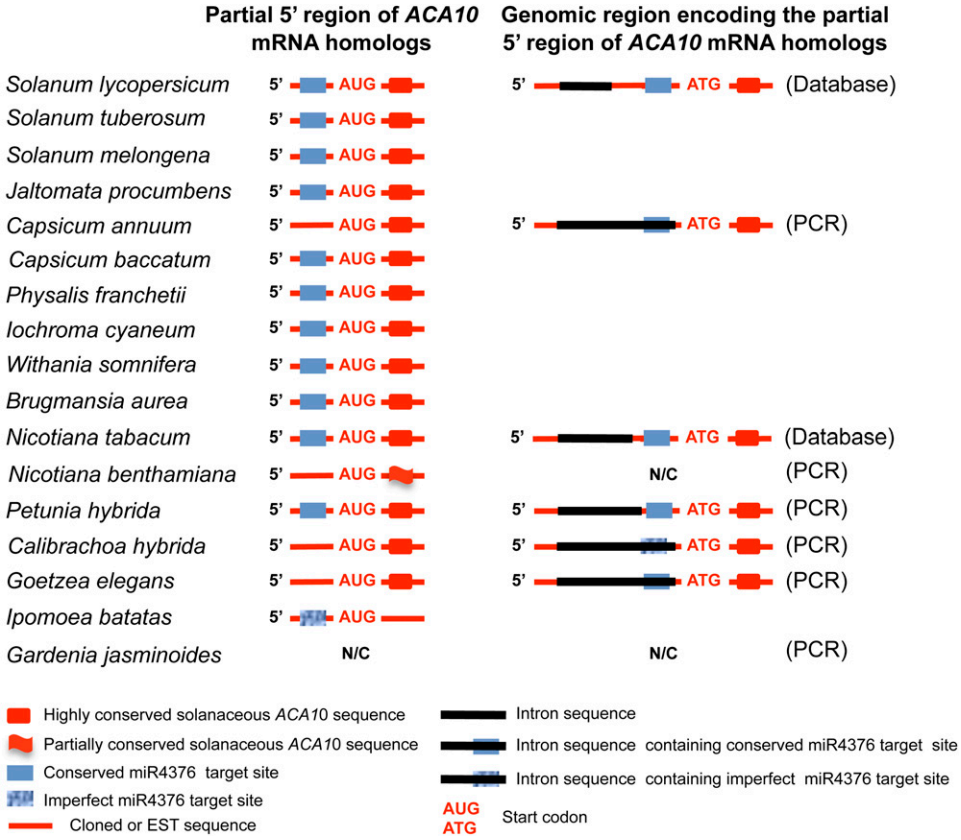

Figure 8. Presence or Absence of the miR4376 Target Site in the 5′-UTRs of *ACA10* Homologs.

The 5′ regions of *ACA10* mRNA homologs were constructed based on partial mRNA sequences obtained from EST databases or 5′-RACE (see Supplemental Table 2 online for details). The genomic region shows embedment of the miR4376 target site within putative introns that is likely spliced out in the mature *ACA10* mRNAs in *C. annuum*, *C. hybrida*, and *G. elegans*. N/C indicates inconclusive results due to difficulty of cloning in 5′-RACE or PCR. The *S. lycopersicum* and *N. tabacum* genomic sequences are available in the databases. For the remaining species, the presence of the miR4376 target site in the genomic sequences of their *ACA10* homologs (not illustrated here) can be inferred based on its presence in the corresponding mRNA homologs.

ACA8 and ACA9 (Baxter et al., 2003). Genetic studies in *A. thaliana* showed that ACA9 is necessary for normal pollen tube growth and fertilization (Schiøtt et al., 2004), and ACA10 is critical for inflorescence growth and juvenile-to-adult phase transition under long-day growth conditions (George et al., 2008). Our data suggest an important role of ACA10 in tomato reproductive growth, adding knowledge to the biological functions of ACAs.

While much has been learned about the regulation of plant Ca^{2+}-ATPase activities and downstream signaling components (Boursiac and Harper, 2007; McAinsh and Pittman, 2009; Dodd et al., 2010; Kudla et al., 2010), how the expression of genes encoding these pumps is regulated remains a major knowledge gap. Studies on a few Ca^{2+}-ATPases from different plant species showed regulation of their expression, as measured by mRNA levels, by salt (Wimmers et al., 1992; Chung et al., 2000), phosphate starvation (Muchhal et al., 1997), cold (Schiøtt and Palmgren, 2005), abscisic acid (Cerana et al., 2006), and fungal elicitor (Chung et al., 2000), but there is no understanding of the molecular mechanisms. Our work uncovered miR4376-regulated *ACA10* expression as an example of a molecular mechanism that regulates the expression of Ca^{2+}-ATPase genes.

Interestingly, the *O. sativa* osa-miR1432 is predicted to target mRNAs of at least three EF hand family proteins (Lu et al., 2008). EF hand proteins function as Ca^{2+} sensors whose conformational change upon Ca^{2+} binding plays critical roles in Ca^{2+}-mediated signaling (DeFalco et al., 2010). Computational analysis predicted a series of human cardiac ion channel/transporter genes, including some Ca^{2+} channels and exchangers, as potential targets of miRNAs (Luo et al., 2010). One of the two isoforms of Serca2 (Serca2b), which encodes a Ca^{2+}-ATPase that pumps Ca^{2+} from the cytosol into the sarco/endoplasmic reticulum in human and mouse muscle cells, contains sites that are targeted by several miRNAs, and its regulation by these miRNAs was confirmed by in vitro studies in human cells with a reporter gene (Salomonis et al., 2010). These observations, together with our experimental work on miR4376-regulated *ACA10* expression, suggest the potentially broader existence of miRNA-mediated Ca^{2+} signaling through modification of the expression levels of certain signaling components.

The production of phased siRNAs from *ACA10* transcripts as a result of miR4376-mediated cleavage raises the intriguing question of whether some, if not all, of such siRNAs would regulate in

trans the expression of certain genes that function as an integrated component of Ca^{2+} signaling pathways or as a separate cellular control mechanism. Addressing this question awaits the validation of the siRNA targets and experimental determination of the biological functions of these targets.

A sRNA-Based Novel Regulatory Mechanism of Tomato Reproductive Growth

It is intriguing that miR4376 mediates the cleavage of *ACA10* mRNA in leaves, but overexpression of miR4376 or *ACA10*^{R} in transgenic tomato plants did not cause visible leaf phenotypes. By contrast, two miRNAs have been demonstrated to play a role in tomato compound leaf development, including miR319, which targets *LANCEOTE* (Ori et al., 2007), and miR164, which targets an mRNA encoding the NAC domain transcription factor, GOBLET (Berger et al., 2009). Several miRNAs and sRNAs are expressed specifically in tomato fruit (Pilcher et al., 2007; Itaya et al., 2008; Moxon et al., 2008). miR159 targets *SGN-U567133*, which encodes a nuclear protein with a NOZZLE-like domain, and transgenic expression of miR159-resistant *SGN-U567133* in tomato leads to pleiotropic developmental defects in leaves, flowers, and fruits (Buxdorf et al., 2010). Our work demonstrates the specific role of a miRNA, and/or perhaps the phased siRNAs produced from the cleaved miRNA target transcripts, in regulating tomato reproduction. Although the basis for the differential effects of miR4376-regulated expression of *ACA10* on vegetative and reproductive development is unclear, these findings are significant in demonstrating that the functional specificity of a miRNA can be regulated at a level beyond target mRNA cleavage in an organ-specific manner. Whether the observed different levels of *ACA10*-derived phased siRNAs in the leaf and flower, based on the deep sequencing data (Figure 2), could partially account for such specificity is an outstanding question.

Our data do not allow us to infer the specific mechanisms of miR4376-regulated *ACA10* expression and/or phased siRNA production in tomato reproductive growth, but some possibilities can be speculated upon. Most wild species of tomato have exerted stigmas (i.e., stigmas protruding beyond their anthers) and are cross-pollinated. During domestication, the styles became recessed (i.e., withdrawn below the anthers), and this was accompanied by increased self-pollination. Chen et al. (2007) recently cloned *Style2.1*, a major quantitative trait locus that regulates style length in association with self-pollination in domesticated tomato. *L02*, the cloned gene responsible for the quantitative trait locus, encodes a putative transcription factor important for cell elongation in developing styles. The transition from exerted to inserted stigma is associated with a mutation in the promoter of *L02* that leads to the downregulated expression of this gene during flower development (Chen et al., 2007). We found that *L02* was not downregulated in our transgenic plants, suggesting that elongated filament growth unlikely involves the function of this gene. Our data suggest that miR4376-regulated *ACA10* expression (and perhaps also phased siRNA production) plays a critical role in regulating stamen filament length, which may be further tested through genetic means. The biological consequence of the elongated stamen filament growth in our transgenic plants remains to be experimentally determined. It also remains to be determined what caused the drastic reduction in fruit yield in these plants. Some possibilities include malfunction of the pollination and/or fertilization process. The small green fruits may result from partial fertilization and embryo abortion, which would inhibit fruit development or cause parthenocarpy.

Multiple Limiting Steps for the Evolution of a miRNA

Our data showed that there were two *MIR4376*-coding loci in all test species below the X=12 clade. The most parsimonious explanation is that there were two versions in the common ancestor of Gardenia (Rubiaceae) and Solanaceae. At some point after the initial diversification of Solanaceae, but after the lineage leading to *Petunia* diverged from that leading to the X=12 clade (*Nicotiana* and all representatives of Solanoideae), one locus was lost (diverged or became silenced) in one or another clade. Our findings demonstrate that deep phylogenetic mapping may allow high-resolution tracing of the evolutionary path of a miRNA that is not deeply conserved in all plants to establish a foundation for further studies on the underlying molecular mechanisms and their biological implications.

We showed that Type III pre-miR4376 transcripts were absent from petunia in repeated RT-PCR experiments. This suggests that either the Type III DNA sequence represents a molecular fossil of a miR4376 ancestor before gaining transcriptional activity or such a transcriptional capacity was lost during the course of evolution. Alternatively, the petunia Type III sequence may be functional now or was so very recently, but at a level that is undetectable, or at a time in plant development that we have not found. On the other hand, the low level of pre-miR4376 transcripts in eggplant may be interpreted as a result of reduced transcription activity of *MIR4376* during evolution. Elucidating the molecular basis of the transcription capacities of *MIR4376* genes in these plants may provide insight into the evolution of *MIR4376* regulatory elements.

Considering the similar accumulation levels of tobacco and tomato pre-miR4376 transcripts, the extremely low level of mature miR4376 in tobacco in comparison with that in tomato is better interpreted as an indication of the poor processing capacity of the tobacco pre-miR4376 transcripts. The nondetectable levels of miR4376 in petunia and *N. benthamiana* may also be due to the poor processing capacity of their precursors. Thus, posttranscriptional processing capacity appears to be a limiting step for the evolution of a miRNA. The mechanistic basis remains to be resolved, but some structural features are notable. The expressed Type II pre-miR4376 in petunia, tobacco, and *N. benthamiana* all have a 4-nucleotide unpaired bulge in the miRNA-miRNA* region, which might disturb processing according to the well-established plant pre-miRNA criteria (Meyers et al., 2008). However, further experiments are necessary to determine the significance of such structural differences. Several recent studies determined the importance of the stem structures distal to the miRNA/miRNA* regions of *Arabidopsis* miR159, miR172a, and miR319 precursors for processing into mature miRNAs (Bologna et al., 2009; Mateos et al., 2010; Song et al., 2010; Werner et al., 2010). We were not able to clone longer sequences, due to difficulty in designing primers, in the corresponding regions of pre-miR4376 from all species for comparisons to better understand the potential structural features

critical for processing. Nevertheless, as a complement to these snapshot views of the *A. thaliana* pre-miRNA structural elements critical for processing, our data provide an evolutionary perspective of structural modifications of a miRNA precursor. This may be useful for future studies to investigate how such structural modifications may impact processing and/or other functions.

Homologs of *ACA10* from different plant species may or may not be the target of a miR4376, depending primarily on (1) whether a homolog carries the target site for the miRNA and (2) whether the mature miRNA is produced at all or at an effective level in a species. Adding to this complexity is the possible splicing event in some plants that affects the fate of a target site in the mature mRNA. Thus, a conserved gene may be regulated by a miRNA in a species-specific manner. The potentially broad importance of alternative splicing in regulating miRNA-target gene interactions is underscored by the finding that exclusion of exons containing miRNA target sites, via alternative splicing, allows Serca2a (an isoform of Serca2) to escape miRNA regulation during cardiac differentiation (Salomonis et al., 2010). This complexity of miRNA-target gene interaction could have significantly impacted the evolution of gene regulation by sRNAs that may function specifically to target transcripts from related family members or others.

Solanaceae as a Model for Experimental Studies on the Evolution and Unique Biological Functions of miRNAs

The low levels of miR4376 in tobacco and other plants may have important evolutionary implications. In an attempt to address this issue, we performed a series of functional analysis in tobacco. We could not detect the miR4376-based cleavage product of *ACA10* in tobacco, suggesting that tobacco miR4376 unlikely regulates *ACA10* expression, at least to a detectable level by current methods. Consistent with this observation, we did not find any phased siRNAs derived from the tobacco *ACA10* in the database (see Supplemental Data Set 1 online). In an attempt to further understand the biological role of miR4376-regulated *ACA10* expression or phased siRNA production, we tried to generate transgenic tobacco plants that overexpress miR4376 under the control of the CaMV 35S promoter but were not able to obtain any plants beyond the callus stage. The data suggest that abundant expression of miR4376 might lead to embryonic or callus-specific lethality to tobacco, providing one piece of experimental evidence to support the postulation that, during miRNA evolution, those miRNAs that may cause lethality to an organism would be eliminated (Fahlgren et al., 2007) (see review in Axtell, 2008). Transgenic expression of miR4376 in *P. hybrida* and eggplant, both having the perfect miR4376-target site in their *ACA10* but having no or low levels of miR4376, respectively, may provide an additional experimental test of this hypothesis. Furthermore, perturbation of miR4376-regulated *ACA10* expression and possibly the associated phased siRNA production in more solanaceous plants, such as eggplant and pepper, may shed additional light on the role of this regulatory mechanism in fruit formation.

In the recent deep sequencing results, over 1000 putative miRNAs found in tomato are not detected in *P. hybrida* (http://smallrna.udel.edu/), suggesting that they have evolved after these species diverged from each other. Expanded studies on the evolutionary mechanisms and biological functions of these miRNAs should significantly advance our general knowledge of miRNA evolution and function.

METHODS

Plant Materials and Growth Conditions

Potato (*Solanum tuberosum*) was obtained from USDA potato gene bank (PI 639205, Sturgeon Bay, WI). Tomato (*Solanum lycopersicum* var Rutgers), *Solanum melongena*, *Jaltomata procumbens*, *Capsicum baccatum*, *Capsicum annuum*, and *Physalis franchetii* were purchased from Trade Winds Fruit. *Petunia hybrida* (Avalanche) was purchased from HPS Horticultural. *Iochroma cyaneum*, *Withania somnifera*, *Brugmansia aurea*, *Calibrachoa hybrida*, *Ipomoea batatas*, *Goetzea elegans*, *Gardenia jasminoides*, and *Chrysanthemum cinerariifolium* were obtained from the Biological Sciences Greenhouse Facility at Ohio State University.

All plants (except *S. tuberosum* and *Arabidopsis thaliana*) were grown in a growth chamber controlled at 14-h light, 27°C/10-h dark, 24°C cycles. *S. tuberosum* and *A. thaliana* were grown in a growth chamber controlled at 16-h light, 22°C/8-h dark, 18°C cycles.

Cloning of Full-Length cDNA of Sl *ACA10* and Constructs for Transformation

We cloned Sl *ACA10* with 3′- and 5′-RACE using a Generacer Kit (Invitrogen) before the tomato genome sequence became available. Forward primers for the initial 3′-RACE were designed to be complementary to the miR4376 sequence with various truncations at the 3′-ends to circumvent mismatch(es) between the miR4376 and target sequence. The reverse primer (i.e., the 3′-RACE adapter-specific primer) was provided in the Generacer kit. Among the forward primers tested, a miR4376 sequence complementary primer (5′-TCCAGCATCATCTCTCCTGCG-3′) that has one nucleotide deletion at the 5′-end of the miR4376 sequence allowed cloning of partial *ACA10* cDNA. The cloned cDNA was identical to an EST sequence (SGN-U371584). Based on the sequence of partial *ACA10*, a new forward primer ACA10 f, 5′-TTGTCAAATCTGGTGTCATCTCTCCTGCG-3′, and a reverse primer Tar5′″″ RACE, 5′-TCCAGCATCATCTCTCCTGCGT-3′, were used for 3′- and 5′-RACE, respectively, for cloning of the full-length *ACA10* cDNA. The full-length *ACA10* cDNA was cloned into pGEMT vector (Promega) for sequencing and pENTR/D/TOPO vector (Invitrogen) for subsequent applications.

To overexpress miR4376, we used expression vector pRS300 that contains a modified miR319 precursor as a backbone to express an artificial miRNA under the control of the CaMV 35S promoter (Schwab et al., 2006). We used overlapping PCR to replace the miR319 sequence with the miR4376 sequence in the backbone. We engineered artificial miRNA vector pRS300-MIR4376 harboring the miR4376 sequence for overexpressing miR4376 in tomato using parental plasmid pRS3000 according to the instructions from http://wmd3.weigelworld.org/cgi-bin/webapp.cgi (Schwab et al., 2006). The parental plasmid pRS300 was a gift from Detlef Weigel (Max Planck Institute, Tübingen, Germany). Primers for this construction are as follows: I amiRMIR4376-s (5′-gaACGCAGGAGAGATGATGCTGGAtctctcttttgtattcc-3′), II amiRMIR4376-a (5′-gaTCCAGCATCATCTCTCCTGCGTtcaaagagaatcaatga-3′), III amiRMIR4376*s (5′-gaTCAAGCATCATCTGTCCTGCGTtcacaggtcgtgatatg-3′), and IV amiRMIR4376*a (5′-gaACGCAGGACAGATGATGCTTGAtctacatatatattcct-3′). The pRS300-MIR4376 construct was used as a backbone to transfer the artificial MIR4376 miRNA region into the pENTR/D/TOPO (Invitrogen) cloning vector using the following primers: CACC-amiRMIR4376-F (5′-caccCTGCAAGGCGATTAAGTTGGGTAAC-3′) and amiRMIR4376-R (5′- GCGGATAACAATTTCACACAGGAAACAG-3′). The resulting plasmid pENTR-MIR4376 construct was recombined with the

pH2GW7 (Karimi et al., 2002) binary vector following instructions from Invitrogen.

To overexpress a mutant Sl *ACA10* with predicted reduced cleavage mediated by miR4376, we inserted the full-length *ACA10* cDNA into the pENTR/D/TOPO vector using modified primers (SlACA10 cacc-C/G f, 5′-caccttgtcaaaTCtgGtgTCATCTATCCTGCG-3′; SlACA10 FLAG r, 5′-ttattaCTTGTCATCGTCGTCCTTGTAGTCTGAACACTCCTGTCGATTTC-TTCG-3′), which changes C at the cleavage site to A. The resulting plasmid, pENTR-C/G-SlACA10, was recombined into the pH2GW7 binary vector by the LR reaction as described above. Constructs expressing GFP as a control were also made.

Transgenic tomato plants overexpressing miR4376-resistant Sl *ACA10* (Sl *ACA10*^{R}), *MIR4376*, or *GFP* were generated at The Ralph M. Parsons Foundation Plant Transformation Facility, University of California at Davis.

Mapping Cleavage Site in Sl *ACA10* mRNA

To map the miR4376 cleavage site in *ACA10* mRNA, the gene-specific primer (MIR4376Tar 5′Race-R, 5′-CCAAATCCTCATTCTGATGCCGCC-TATACG-3′) was used in modified 5′-RACE as previously described (Llave et al., 2002; Kasschau et al., 2003). 5′-RACE was performed using the GeneRACER kit from Invitrogen using RNA samples isolated from tomato flowers and leaves.

Cloning of the miRNA Target Site

To clone the miR4376 target site from solanaceous species and *I. batatas*, the primer ACA10 all universal f (5′-CTTAATGCTTCTCGTCGATTTCGA-TATAC-3′) was used, in addition to the 5′-RACE–specific primer from the Generacer kit (Invitrogen). For details, see Supplemental Figure 12 online. The PCR products were ligated into TA Cloning Kit from Invitrogen following the manufacturer's instructions. The clone was sequenced at the Plant-Microbe Genomic Facility at Ohio State University.

Cloning of *MIR4376*-Containing DNA Sequences and miR4376-Containing Precursor Transcripts

To clone DNA sequences containing *MIR4376* from the genomes of different species, the DNAeasy plant mini kit (Qiagen) was used to purify the genomic DNAs following the manufacturer's instructions. Primers (MIR4376 f, 5′-AAGGCTTGCTACGCAGGAGA-3′; MIR4376 r, 5′-AGGCT-TAATATGCAGGAGTATGATGCTG-3′) were used for PCR using genomic DNA as templates (Genome PCR). The PCR fragments were ligated into pGEM-T vector (Promega) and sequenced as described above.

To clone miR4376 precursor transcripts, RNA samples were prepared using the Ribozol Plus RNA purification kit (Amresco) followed by RT-PCR using Superscript III reverse transcriptase (Invitrogen) and FideliTaq polymerase (USB). The PCR products were inserted into the pGEM-T vector (Promega) and sequenced as described above. PCR without RT showed no amplified products, ruling out the possibility of genomic DNA contamination in the RNA samples.

Total RNA Isolation and Enrichment for sRNAs

Total RNA from leaves or flowers (1 g of fresh weight) was isolated using Trizol reagent (Invitrogen). sRNA species were enriched using the mirVana miRNA isolation kit (Ambion) following the manufacturer's instructions. The RNA sample from each species was divided equally into two halves, one for the detection of miR4376 and the other for the detection of miR166 (internal control; see below).

RNA Expression Analysis

For detection of miR4376 and miR166 via RNA gel blotting, 1 to 5 μg of enriched sRNAs (see above) was separated on 17% (w/v) polyacrylamide/8 M urea–0.5× Tris/Borate/EDTA gel and transferred to a Hybond-XL nylon membrane (Amersham Biosciences) and UV cross-linked. The membranes were hybridized in ULTRAhyb ultrasensitive hybridization buffer (Ambion) overnight with miRNA-specific probes, which were prepared by 5′-end labeling synthetic DNA oligos (IDT) complementary to the miR4376 (probe sequence is 5′-TCCAGCATCATCTCTCCTGCGT-3′) and miR166 (probe sequence is 5′-GGGGAATGAAGCCTGGTCCGA-3′) sequences, respectively, as described in detail by Wang et al. (2007b). After hybridization, the membranes were washed once in 2× SSC (1× SSC is 0.15 M NaCl plus 0.015 M sodium citrate), 0.1% sodium SDS for 10 min, and washed once in 0.2× SSC, 0.1% SDS for 10 min. Hybridization and washing were performed at 37.5°C. The washed membranes were exposed to storage phosphor screens (Kodak). The screen was scanned by Molecular Imager FX using Quantity One-4.1.1 software (Bio-Rad).

For RT-PCR analysis of *ACA10* and *ACA10*^{R} transcripts in the *ACA10*^{R} overexpression lines, we used a primer set (forward, 5′-CGGTGATGA-AGGCGATAAACCCTAG-3′; reverse, 5′-GTATATCGAAATCGACGAGG-AGCATTAAG-3′) for endogenous *ACA10* and a primer set (35S forward, 5′-CGCAAGACCCTTCCTCTATATAAGG-3′; reverse, 5′-GTATATCGAA-ATCGACGAGGAGCATTAAG-3′) for *ACA10*^{R}. These two different primer sets will distinguish the endogenous (*ACA10*) and exogenous (*ACA10*^{R}) transcripts.

Yeast Transformation

Yeast strains W303 (*MAT***a**, *leu2, his3, ade2, trp1, ura3*) and K616 (*MAT***a** *pmr1*::*HIS3 pmc1*::*TRP1 cnb1*::*LEU2, ura3*) were described previously (Cunningham and Fink, 1994). Both yeast strains are gifts from Heven Sze at the University of Maryland. *FLAG-SlACA10*^{R} was used to transform the K616 strain as described by Liang et al. (1997). Yeasts were grown in YPD medium (yeast extract/peptone/dextrose) except for the K616 transformants that were additionally supplied with 10 mM $CaCl_2$ after transformation.

Accession Numbers

Sequence data from this article can be found in the Arabidopsis Genome Initiative or GenBank/EMBL databases under the following accession numbers: AT4G29900.1 (At *ACA10*), JN580452 (Sl *ACA10*), and JN603461 (Sly-miR4376). The accession numbers for Gma-miR4376 and its precursor are MIMAT0018280 and MI0016521, respectively, in the miRBase (http://www.mirbase.org/).

Supplemental Data

The following materials are available in the online version of this article.

Supplemental Figure 1. Leaf Position-Dependent Expression of miR4376 in Tomato, Shown by RNA Gel Blots.

Supplemental Figure 2. Alignment of At ACA10 and Sl ACA10 Protein Sequences.

Supplemental Figure 3. Immunoblots to Detect the Accumulation of Transgenically Expressed GFP and ACA10 Proteins in Tomato Plants.

Supplemental Figure 4. Overexpression of miR4376 or Sl *ACA10*^{R} in Transgenic Tomato Plants Has No Visible Effect on Germination or Leaf Morphology.

Supplemental Figure 5. Quantitative Measurements Showing Stamen Filament Overgrowth in miR4376-OX and SlACA10^R-OX Tomato Plants.

Supplemental Figure 6. Young Fruits on a miR4376-OX Plant and an SlACA10^R-OX Plant That Will Not Grow Further.

Supplemental Figure 7. A Simplified Phylogeny Tree of Plants Based on Chase and Reveal (2009) to Show Presence or Absence of miR4376.

Supplemental Figure 8. Sequences and Secondary Structures of Two Versions of miR4376 from *Chrysanthemum cinerariifolium*.

Supplemental Figure 9. RNA Gel Blot Showing Presence of miR4376 in Tomato but Absence in Several Other Plant Species.

Supplemental Figure 10. Primer Design for Cloning miR4376-Coding DNA Sequences and Precursor Transcripts from Different Plant Species.

Supplemental Figure 11. Sequences of miR4376 Precursors Computationally Transcribed from Cloned Genomic Sequences and the Predicted Secondary Structures from Various Species, Corresponding to Those Illustrated Schematically in Figure 4.

Supplemental Figure 12. Flow Chart Showing the Strategies for RACE and Genomic Cloning to Amplify the Corresponding 5′-UTR Sequences of *ACA10* Orthologs in the mRNA Transcripts and Genomic Regions, Respectively.

Supplemental Figure 13. cDNA Sequences of *ACA10* 5′-UTR Regions from Various Species.

Supplemental Figure 14. The Genomic Sequences Flanking the 5′-UTR Region Harboring a Similar or Identical miR4376 Target Site.

Supplemental Figure 15. Phased siRNAs Derived from Potato *ACA10* Based on Searches in the Small RNA Deep Sequencing Database (http://smallrna.udel.edu/).

Supplemental Figures 16. Presence of the miR4376 Target Site-Like Sequence at the Equivalent Positions of the 5′-UTRs of *ACA10* Homologs in Several Plant Species Distantly Related to Solanaceous Plants.

Supplemental Table 1. Deep Sequencing Counts of miR4376 from the Open Source Database of Comparative Sequencing of Plant Small RNAs (http://smallrna.udel.edu/project_data.php).

Supplemental Table 2. Summary of Methods Used to Obtain miR4376 Target Site Information from Different Plant Species and Results.

Supplemental Data Set 1. Summary of Small RNAs Mapped to the *ACA10* Transcripts in *S. lycopersicum*, *S. tuberosum*, *C. annuum*, *N. tabacum*, and *P. hybrida* Obtained from Searches in the Small RNA Database (http://smallrna.udel.edu/).

Supplemental Data Set 2. Computational Prediction for the Target Genes of the Tomato Phased siRNAs 3′ P2+ (Small RNA ID S0943954) and 3′ P5+ (Small RNA ID S0418649).

Supplemental Data Set 3. Search Results for Small RNAs Similar to miR4376 and Their Genomic Loci.

ACKNOWLEDGMENTS

We thank Elizabeth Luscher for plant maintenance and technical assistance, Ryuta Takeda and Xiaorui Yang for valuable suggestions and critical reading of this manuscript, and Sam Griffiths-Jones for advice on the miRNA nomenclature. We also thank the anonymous reviewers for their constructive criticisms and suggestions. We gratefully acknowledge the many insights provided by coeditor Blake Meyers, particularly his suggestion and advice for us to analyze the possibility of miR4376-triggered formation of phased siRNAs from *ACA10*. This work was supported by grants from the National Research Initiative of the USDA Cooperative State Research, Education, and Extension Service (2004-35304-15005), the Ohio Plant Biotechnology Consortium, and in part by a grant from the U.S. National Science Foundation (IOB-0840906).

AUTHOR CONTRIBUTIONS

Y. Wang and B.D. designed the research, analyzed the data, and wrote the article. Y. Wang, A.I., and X.Z. designed the research, performed the research, and analyzed the data. Y. Wu performed the research and analyzed the data. E.v.d.K., R.O., and Y.Q. analyzed the data. J.Z. performed the research.

Received June 6, 2011; revised August 12, 2011; accepted August 26, 2011; published September 13, 2011.

REFERENCES

Ahn, D.H., Singaravelu, G., Lee, S., Ahnn, J., and Shim, Y.H. (2006). Functional and phenotypic relevance of differentially expressed proteins in calcineurin mutants of *Caenorhabditis elegans*. Proteomics **6:** 1340–1350.

Allen, E., Xie, Z., Gustafson, A.M., and Carrington, J.C. (2005). microRNA-directed phasing during trans-acting siRNA biogenesis in plants. Cell **121:** 207–221.

Allen, E., Xie, Z., Gustafson, A.M., Sung, G.H., Spatafora, J.W., and Carrington, J.C. (2004). Evolution of microRNA genes by inverted duplication of target gene sequences in *Arabidopsis thaliana*. Nat. Genet. **36:** 1282–1290.

Axtell, M.J. (2008). Evolution of microRNAs and their targets: are all microRNAs biologically relevant? Biochim. Biophys. Acta **1779:** 725–734.

Axtell, M.J., and Bowman, J.L. (2008). Evolution of plant microRNAs and their targets. Trends Plant Sci. **13:** 343–349.

Axtell, M.J., Snyder, J.A., and Bartel, D.P. (2007). Common functions for diverse small RNAs of land plants. Plant Cell **19:** 1750–1769.

Barakat, A., Wall, K., Leebens-Mack, J., Wang, Y.J., Carlson, J.E., and Depamphilis, C.W. (2007). Large-scale identification of microRNAs from a basal eudicot (*Eschscholzia californica*) and conservation in flowering plants. Plant J. **51:** 991–1003.

Basu, S., and Briskin, D.P. (1995). Target molecular size suggesting a dimeric structure for the red beet plasma membrane Ca^{2+}-ATPase. Phytochemistry **38:** 15–17.

Baxter, I., Tchieu, J., Sussman, M.R., Boutry, M., Palmgren, M.G., Gribskov, M., Harper, J.F., and Axelsen, K.B. (2003). Genomic comparison of P-type ATPase ion pumps in *Arabidopsis* and rice. Plant Physiol. **132:** 618–628.

Berger, Y., Harpaz-Saad, S., Brand, A., Melnik, H., Sirding, N., Alvarez, J.P., Zinder, M., Samach, A., Eshed, Y., and Ori, N. (2009). The NAC-domain transcription factor GOBLET specifies leaflet boundaries in compound tomato leaves. Development **136:** 823–832.

Bologna, N.G., Mateos, J.L., Bresso, E.G., and Palatnik, J.F. (2009). A loop-to-base processing mechanism underlies the biogenesis of plant microRNAs miR319 and miR159. EMBO J. **28:** 3646–3656.

Bonza, M.C., Morandini, P., Luoni, L., Geisler, M., Palmgren, M.G., and De Michelis, M.I. (2000). At-ACA8 encodes a plasma membrane-localized calcium-ATPase of Arabidopsis with a calmodulin-binding domain at the N terminus. Plant Physiol. **123:** 1495–1506.

Boursiac, Y., and Harper, J.F. (2007). The origin and function of calmodulin regulated Ca^{2+} pumps in plants. J. Bioenerg. Biomembr. **39:** 409–414.

Buxdorf, K., Hendelman, A., Stav, R., Lapidot, M., Ori, N., and Arazi,

T. (2010). Identification and characterization of a novel miR159 target not related to MYB in tomato. Planta **232:** 1009–1022.

Carafoli, E. (2002). Calcium signaling: a tale for all seasons. Proc. Natl. Acad. Sci. USA **99:** 1115–1122.

Carthew, R.W., and Sontheimer, E.J. (2009). Origins and mechanisms of miRNAs and siRNAs. Cell **136:** 642–655.

Cerana, M., Bonza, M.C., Harris, R., Sanders, D., and De Michelis, M.I. (2006). Abscisic acid stimulates the expression of two isoforms of plasma membrane Ca^{2+}-ATPase in *Arabidopsis thaliana* seedlings. Plant Biol. (Stuttg.) **8:** 572–578.

Chase, M.W., and Reveal, J.L. (2009). A phylogenetic classification of the land plants to accompany APG III. Bot. J. Linn. Soc. **161:** 122–127.

Chen, H.M., Chen, L.T., Patel, K., Li, Y.H., Baulcombe, D.C., and Wu, S.H. (2010). 22-Nucleotide RNAs trigger secondary siRNA biogenesis in plants. Proc. Natl. Acad. Sci. USA **107:** 15269–15274.

Chen, K.-Y., Cong, B., Wing, R., Vrebalov, J., and Tanksley, S.D. (2007). Changes in regulation of a transcription factor lead to autogamy in cultivated tomatoes. Science **318:** 643–645.

Chen, X. (2009). Small RNAs and their roles in plant development. Annu. Rev. Cell Dev. Biol. **25:** 21–44.

Chung, W.S., Lee, S.H., Kim, J.C., Heo, W.D., Kim, M.C., Park, C.Y., Park, H.C., Lim, C.O., Kim, W.B., Harper, J.F., and Cho, M.J. (2000). Identification of a calmodulin-regulated soybean $Ca^{(2+)}$-ATPase (SCA1) that is located in the plasma membrane. Plant Cell **12:** 1393–1407.

Cunningham, K., and Fink, G. (1994). Calcineurin-dependent growth control in *Saccharomyces cerevisiae* mutants lacking *PMC1*, a homolog of plasma membrane Ca^{2+} ATPases. J. Cell Biol. **124:** 351–363.

Cuperus, J.T., Carbonell, A., Fahlgren, N., Garcia-Ruiz, H., Burke, R.T., Takeda, A., Sullivan, C.M., Gilbert, S.D., Montgomery, T.A., and Carrington, J.C. (2010). Unique functionality of 22-nt miRNAs in triggering RDR6-dependent siRNA biogenesis from target transcripts in Arabidopsis. Nat. Struct. Mol. Biol. **17:** 997–1003.

Cuperus, J.T., Fahlgren, N., and Carrington, J.C. (2011). Evolution and functional diversification of MIRNA genes. Plant Cell **23:** 431–442.

DeFalco, T.A., Bender, K.W., and Snedden, W.A. (2010). Breaking the code: Ca^{2+} sensors in plant signalling. Biochem. J. **425:** 27–40.

Dodd, A.N., Kudla, J., and Sanders, D. (2010). The language of calcium signaling. Annu. Rev. Plant Biol. **61:** 593–620.

Fahlgren, N., Howell, M.D., Kasschau, K.D., Chapman, E.J., Sullivan, C.M., Cumbie, J.S., Givan, S.A., Law, T.F., Grant, S.R., Dangl, J.L., and Carrington, J.C. (2007). High-throughput sequencing of *Arabidopsis* microRNAs: Evidence for frequent birth and death of *MIRNA* genes. PLoS ONE **2:** e219.

Fahlgren, N., Jogdeo, S., Kasschau, K.D., Sullivan, C.M., Chapman, E.J., Laubinger, S., Smith, L.M., Dasenko, M., Givan, S.A., Weigel, D., and Carrington, J.C. (2010). MicroRNA gene evolution in *Arabidopsis lyrata* and *Arabidopsis thaliana*. Plant Cell **22:** 1074–1089.

Felippes, F.F., Schneeberger, K., Dezulian, T., Huson, D.H., and Weigel, D. (2008). Evolution of *Arabidopsis thaliana* microRNAs from random sequences. RNA **14:** 2455–2459.

Floyd, S.K., and Bowman, J.L. (2004). Gene regulation: Ancient microRNA target sequences in plants. Nature **428:** 485–486.

Geisler, M., Axelsen, K.B., Harper, J.F., and Palmgren, M.G. (2000). Molecular aspects of higher plant P-type $Ca^{(2+)}$-ATPases. Biochim. Biophys. Acta **1465:** 52–78.

George, L., Romanowsky, S.M., Harper, J.F., and Sharrock, R.A. (2008). The ACA10 Ca^{2+}-ATPase regulates adult vegetative development and inflorescence architecture in *Arabidopsis*. Plant Physiol. **146:** 716–728.

Hardingham, G.E., and Bading, H. (2003). The Yin and Yang of NMDA receptor signalling. Trends Neurosci. **26:** 81–89.

Hepler, P.K. (2005). Calcium: A central regulator of plant growth and development. Plant Cell **17:** 2142–2155.

Itaya, A., Bundschuh, R., Archual, A.J., Joung, J.G., Fei, Z., Dai, X., Zhao, P.X., Tang, Y., Nelson, R.S., and Ding, B. (2008). Small RNAs in tomato fruit and leaf development. Biochim. Biophys. Acta **1779:** 99–107.

Johnson, C., Kasprzewska, A., Tennessen, K., Fernandes, J., Nan, G.L., Walbot, V., Sundaresan, V., Vance, V., and Bowman, L.H. (2009). Clusters and superclusters of phased small RNAs in the developing inflorescence of rice. Genome Res. **19:** 1429–1440.

Joshi, T., Yan, Z., Libault, M., Jeong, D.H., Park, S., Green, P.J., Sherrier, D.J., Farmer, A., May, G., Meyers, B.C., Xu, D., and Stacey, G. (2010). Prediction of novel miRNAs and associated target genes in Glycine max. BMC Bioinformatics **11**(Suppl. 1): S14.

Karimi, M., Inzé, D., and Depicker, A. (2002). GATEWAY vectors for Agrobacterium-mediated plant transformation. Trends Plant Sci. **7:** 193–195.

Kasschau, K.D., Xie, Z.X., Allen, E., Llave, C., Chapman, E.J., Krizan, K.A., and Carrington, J.C. (2003). P1/HC-Pro, a viral suppressor of RNA silencing, interferes with *Arabidopsis* development and miRNA unction. Dev. Cell **4:** 205–217.

Kim, V.N., Han, J., and Siomi, M.C. (2009). Biogenesis of small RNAs in animals. Nat. Rev. Mol. Cell Biol. **10:** 126–139.

Kudla, J., Batistic, O., and Hashimoto, K. (2010). Calcium signals: The lead currency of plant information processing. Plant Cell **22:** 541–563.

Kurihara, Y., Takashi, Y., and Watanabe, Y. (2006). The interaction between DCL1 and HYL1 is important for efficient and precise processing of pri-miRNA in plant microRNA biogenesis. RNA **12:** 206–212.

Kurihara, Y., and Watanabe, Y. (2004). *Arabidopsis* micro-RNA biogenesis through Dicer-like 1 protein functions. Proc. Natl. Acad. Sci. USA **101:** 12753–12758.

Kutter, C., Schöb, H., Stadler, M., Meins, F., Jr., and Si-Ammour, A. (2007). MicroRNA-mediated regulation of stomatal development in *Arabidopsis*. Plant Cell **19:** 2417–2429.

Lelandais-Brière, C., Naya, L., Sallet, E., Calenge, F., Frugier, F., Hartmann, C., Gouzy, J., and Crespi, M. (2009). Genome-wide *Medicago truncatula* small RNA analysis revealed novel microRNAs and isoforms differentially regulated in roots and nodules. Plant Cell **21:** 2780–2796.

Li, D., Wang, L., Wang, M., Xu, Y.Y., Luo, W., Liu, Y.J., Xu, Z.H., Li, J., and Chong, K. (2009). Engineering OsBAK1 gene as a molecular tool to improve rice architecture for high yield. Plant Biotechnol. J. **7:** 791–806.

Liang, F., Cunningham, K.W., Harper, J.F., and Sze, H. (1997). ECA1 complements yeast mutants defective in Ca^{2+} pumps and encodes an endoplasmic reticulum-type Ca^{2+}-ATPase in *Arabidopsis thaliana*. Proc. Natl. Acad. Sci. USA **94:** 8579–8584.

Llave, C., Xie, Z., Kasschau, K.D., and Carrington, J.C. (2002). Cleavage of *Scarecrow-like* mRNA targets directed by a class of *Arabidopsis* miRNA. Science **297:** 2053–2056.

Lu, C., et al. (2008). Genome-wide analysis for discovery of rice microRNAs reveals natural antisense microRNAs (nat-miRNAs). Proc. Natl. Acad. Sci. USA **105:** 4951–4956.

Lu, C., Kulkarni, K., Souret, F.F., MuthuValliappan, R., Tej, S.S., Poethig, R.S., Henderson, I.R., Jacobsen, S.E., Wang, W., Green, P.J., and Meyers, B.C. (2006). MicroRNAs and other small RNAs enriched in the *Arabidopsis* RNA-dependent RNA polymerase-2 mutant. Genome Res. **16:** 1276–1288.

Lu, S., Sun, Y.H., Shi, R., Clark, C., Li, L., and Chiang, V.L. (2005). Novel and mechanical stress-responsive MicroRNAs in *Populus*

trichocarpa that are absent from *Arabidopsis*. Plant Cell **17:** 2186–2203.

Luo, X.B., Zhang, H.J., Xiao, J.N., and Wang, Z.G. (2010). Regulation of human cardiac ion channel genes by microRNAs: Theoretical perspective and pathophysiological implications. Cell. Physiol. Biochem. **25:** 571–586.

Ma, Z., Coruh, C., and Axtell, M.J. (2010). *Arabidopsis lyrata* small RNAs: Transient MIRNA and small interfering RNA loci within the *Arabidopsis* genus. Plant Cell **22:** 1090–1103.

Mahalingam, G., and Meyers, B.C. (2009). Computational methods for comparative analysis of plant small RNAs. In Plant MicroRNAs, Methods in Molecular Biology, B.C.M.a.P.J. Green, ed (New York: Humana Press), pp. 163–181.

Mallory, A.C., Reinhart, B.J., Jones-Rhoades, M.W., Tang, G., Zamore, P.D., Barton, M.K., and Bartel, D.P. (2004). MicroRNA control of PHABULOSA in leaf development: Importance of pairing to the microRNA 5′ region. EMBO J. **23:** 3356–3364.

Mateos, J.L., Bologna, N.G., Chorostecki, U., and Palatnik, J.F. (2010). Identification of microRNA processing determinants by random mutagenesis of Arabidopsis MIR172a precursor. Curr. Biol. **20:** 49–54.

McAinsh, M.R., and Pittman, J.K. (2009). Shaping the calcium signature. New Phytol. **181:** 275–294.

Meyers, B.C., et al. (2008). Criteria for annotation of plant microRNAs. Plant Cell **20:** 3186–3190.

Molnár, A., Schwach, F., Studholme, D.J., Thuenemann, E.C., and Baulcombe, D.C. (2007). miRNAs control gene expression in the single-cell alga *Chlamydomonas reinhardtii*. Nature **447:** 1126–1129.

Montgomery, T.A., Yoo, S.J., Fahlgren, N., Gilbert, S.D., Howell, M.D., Sullivan, C.M., Alexander, A., Nguyen, G., Allen, E., Ahn, J.H., and Carrington, J.C. (2008). AGO1-miR173 complex initiates phased siRNA formation in plants. Proc. Natl. Acad. Sci. USA **105:** 20055–20062.

Morin, R.D., Aksay, G., Dolgosheina, E., Ebhardt, H.A., Magrini, V., Mardis, E.R., Sahinalp, S.C., and Unrau, P.J. (2008). Comparative analysis of the small RNA transcriptomes of *Pinus contorta* and *Oryza sativa*. Genome Res. **18:** 571–584.

Moxon, S., Jing, R., Szittya, G., Schwach, F., Rusholme Pilcher, R.L., Moulton, V., and Dalmay, T. (2008). Deep sequencing of tomato short RNAs identifies microRNAs targeting genes involved in fruit ripening. Genome Res. **18:** 1602–1609.

Muchhal, U.S., Liu, C.M., and Raghothama, K.G. (1997). Ca^{2+}-ATPase is expressed differentially in phosphate-starved roots of tomato. Physiol. Plant. **101:** 540–544.

Okada, C., Yamashita, E., Lee, S.J., Shibata, S., Katahira, J., Nakagawa, A., Yoneda, Y., and Tsukihara, T. (2009). A high-resolution structure of the pre-microRNA nuclear export machinery. Science **326:** 1275–1279.

Olmstead, R., Bohs, L., Migid, H., Santiago-Valentin, E., Garcia, V., and Collier, S. (2008). A molecular phylogeny of the Solanaceae. Taxon **57:** 1159–1181.

Olmstead, R.G., Kim, K.J., Jansen, R.K., and Wagstaff, S.J. (2000). The phylogeny of the Asteridae sensu lato based on chloroplast ndhF gene sequences. Mol. Phylogenet. Evol. **16:** 96–112.

Ori, N., et al. (2007). Regulation of LANCEOLATE by miR319 is required for compound-leaf development in tomato. Nat. Genet. **39:** 787–791.

Park, W., Li, J., Song, R., Messing, J., and Chen, X. (2002). CARPEL FACTORY, a Dicer homolog, and HEN1, a novel protein, act in microRNA metabolism in *Arabidopsis thaliana*. Curr. Biol. **12:** 1484–1495.

Pilcher, R.L.R., Moxon, S., Pakseresht, N., Moulton, V., Manning, K., Seymour, G., and Dalmay, T. (2007). Identification of novel small RNAs in tomato (*Solanum lycopersicum*). Planta **226:** 709–717.

Rajagopalan, R., Vaucheret, H., Trejo, J., and Bartel, D.P. (2006). A diverse and evolutionarily fluid set of microRNAs in *Arabidopsis thaliana*. Genes Dev. **20:** 3407–3425.

Reinhart, B.J., Weinstein, E.G., Rhoades, M.W., Bartel, B., and Bartel, D.P. (2002). MicroRNAs in plants. Genes Dev. **16:** 1616–1626.

Sackett, D.L., and Kosk-Kosicka, D. (1996). The active species of plasma membrane Ca^{2+}-ATPase are a dimer and a monomer-calmodulin complex. J. Biol. Chem. **271:** 9987–9991.

Salomonis, N., et al. (2010). Alternative splicing regulates mouse embryonic stem cell pluripotency and differentiation. Proc. Natl. Acad. Sci. USA **107:** 10514–10519.

Sanders, D., Brownlee, C., and Harper, J.F. (1999). Communicating with calcium. Plant Cell **11:** 691–706.

Sanders, D., Pelloux, J., Brownlee, C., and Harper, J.F. (2002). Calcium at the crossroads of signaling. Plant Cell **14**(Suppl): S401–S417.

Schiøtt, M., and Palmgren, M.G. (2005). Two plant Ca2+ pumps expressed in stomatal guard cells show opposite expression patterns during cold stress. Physiol. Plant. **124:** 278–283.

Schiøtt, M., Romanowsky, S.M., Baekgaard, L., Jakobsen, M.K., Palmgren, M.G., and Harper, J.F. (2004). A plant plasma membrane Ca^{2+} pump is required for normal pollen tube growth and fertilization. Proc. Natl. Acad. Sci. USA **101:** 9502–9507.

Schwab, R., Ossowski, S., Riester, M., Warthmann, N., and Weigel, D. (2006). Highly specific gene silencing by artificial microRNAs in *Arabidopsis*. Plant Cell **18:** 1121–1133.

Song, L., Axtell, M.J., and Fedoroff, N.V. (2010). RNA secondary structural determinants of miRNA precursor processing in *Arabidopsis*. Curr. Biol. **20:** 37–41.

Sunkar, R., and Jagadeeswaran, G. (2008). In silico identification of conserved microRNAs in large number of diverse plant species. BMC Plant Biol. **8:** 37.

Sze, H., Liang, F., Hwang, I., Curran, A.C., and Harper, J.F. (2000). Diversity and regulation of plant Ca^{2+} pumps: Insights from expression in yeast. Annu. Rev. Plant Physiol. Plant Mol. Biol. **51:** 433–462.

Szittya, G., Moxon, S., Santos, D.M., Jing, R., Fevereiro, M.P., Moulton, V., and Dalmay, T. (2008). High-throughput sequencing of *Medicago truncatula* short RNAs identifies eight new miRNA families. BMC Genomics **9:** 593.

Ushimaru, M., and Fukushima, Y. (2008). The dimeric form of Ca^{2+}-ATPase is involved in Ca^{2+} transport in the sarcoplasmic reticulum. Biochem. J. **414:** 357–361.

Voinnet, O. (2009). Origin, biogenesis, and activity of plant microRNAs. Cell **136:** 669–687.

Wang, L., Xu, Y.Y., Li, J., Powell, R.A., Xu, Z.H., and Chong, K. (2007a). Transgenic rice plants ectopically expressing AtBAK1 are semi-dwarfed and hypersensitive to 24-epibrassinolide. J. Plant Physiol. **164:** 655–664.

Wang, Y., Zhong, X., Itaya, A., and Ding, B. (2007b). Evidence for the existence of the loop E motif of *Potato spindle tuber viroid* in vivo. J. Virol. **81:** 2074–2077.

Wei, B., Cai, T., Zhang, R., Li, A., Huo, N., Li, S., Gu, Y.Q., Vogel, J., Jia, J., Qi, Y., and Mao, L. (2009). Novel microRNAs uncovered by deep sequencing of small RNA transcriptomes in bread wheat (*Triticum aestivum L.*) and *Brachypodium distachyon* (L.) Beauv. Funct. Integr. Genomics **9:** 499–511.

Werner, S., Wollmann, H., Schneeberger, K., and Weigel, D. (2010). Structure determinants for accurate processing of miR172a in *Arabidopsis thaliana*. Curr. Biol. **20:** 42–48.

Wimmers, L.E., Ewing, N.N., and Bennett, A.B. (1992). Higher plant

Ca(2+)-ATPase: Primary structure and regulation of mRNA abundance by salt. Proc. Natl. Acad. Sci. USA **89:** 9205–9209.

Yoshikawa, M., Peragine, A., Park, M.Y., and Poethig, R.S. (2005). A pathway for the biogenesis of trans-acting siRNAs in Arabidopsis. Genes Dev. **19:** 2164–2175.

Zhang, B., Wang, Q., and Pan, X. (2007). MicroRNAs and their regulatory roles in animals and plants. J. Cell. Physiol. **210:** 279–289.

Zhao, T., Li, G., Mi, S., Li, S., Hannon, G.J., Wang, X.J., and Qi, Y. (2007). A complex system of small RNAs in the unicellular green alga *Chlamydomonas reinhardtii*. Genes Dev. **21:** 1190–1203.

Zhu, Q.H., Spriggs, A., Matthew, L., Fan, L., Kennedy, G., Gubler, F., and Helliwell, C. (2008). A diverse set of microRNAs and microRNA-like small RNAs in developing rice grains. Genome Res. **18:** 1456–1465.

Zuker, M. (2003). Mfold web server for nucleic acid folding and hybridization prediction. Nucleic Acids Res. **31:** 3406–3415.

Function and Evolution of a MicroRNA That Regulates a Ca^{2+}-ATPase and Triggers the Formation of Phased Small Interfering RNAs in Tomato Reproductive Growth

Ying Wang, Asuka Itaya, Xuehua Zhong, Yang Wu, Jianfeng Zhang, Esther van der Knaap, Richard Olmstead, Yijun Qi and Biao Ding

Plant Cell 2011;23;3185-3203; originally published online September 13, 2011;
DOI 10.1105/tpc.111.088013